SVERIGES GEOLOGISKA UNDERSÖKNING

SERIE C NR 817 AVHANDLINGAR OCH UPPSATSER ÅRSBOK 81 NR 3

BJØRN HAGESKOV

# THOLEIITIC DYKES AND THEIR CHEMICAL ALTERATION DURING AMPHIBOLITE FACIES METAMORPHISM: THE KATTSUND-KOSTER DYKE SWARM SE NORWAY — W SWEDEN

UPPSALA 1987

SVERIGES GEOLOGISKA UNDERSÖKNING

SERIE C NR 817 AVHANDLINGAR OCH UPPSATSER ÅRSBOK 81 NR 3

BJØRN HAGESKOV

# THOLEIITIC DYKES AND THEIR CHEMICAL ALTERATION DURING AMPHIBOLITE FACIES METAMORPHISM: THE KATTSUND-KOSTER DYKE SWARM SE NORWAY — W SWEDEN

UPPSALA 1987

ISBN 91-7158-413-7
ISSN 0082-0024

Address:
Bjørn Hageskov
Institut for almen Geologi
Københavns Universitet
Østervoldgade 10
DK-1350 København K, Danmark

Fotosats: ORD & FORM AB
Tryck: Offsetcenter ab, Uppsala 1987

## CONTENTS

Abstract ..... 4
Introduction ..... 4
The Koster dyke swarm ..... 6
Description of the dykes within the sectors ..... 7
The Kattsund dykes ..... 8
Petrography ..... 9
The Sandbukta gneiss ..... 10
Geochemistry ..... 11
Sampling of the dykes ..... 11
The pre-metamorphic chemistry of the dyke swarms ..... 12
Samples from the dyke centres ..... 12
Primary (?) chemical variation between chilled margin and dyke centre ..... 17
Profile across a Koster dyke ..... 19
The protected Kattsund dykes ..... 19
Comments to the chemistry of the Kattsund dykes ..... 19
The evolution of the Koster and the Kattsund dyke magmas ..... 20
Chemical differences between Koster dykes from sector I, II and III ..... 25
Comparison of the mean dyke compositions of sector I, II and III ..... 26
Comparing the individual sector II and III samples to the magmatic trends of the sector I dykes ..... 26
Conclusion ..... 27
Chemical alteration in the marginal zone of the Kattsund dykes ..... 27
Profiles across Kattsund dykes ..... 27
The marginal zone of the profiles ..... 33
The paired samples ..... 33
Conclusion on the study of the alterations in the Kattsund dykes ..... 39
Comparison of the metasomatic changes of the Kattsund and the Koster dykes with other metasomatically altered basic dyke rocks ..... 40
Acknowledgements ..... 42
Appendix ..... 43
Analytical methods etc. ..... 43
Tables ..... 44
References ..... 60

## ABSTRACT

Bjørn Hageskov: Tholeiitic dykes and their chemical alteration during amphibolite facies metamorphism: the Kattsund-Koster dyke swarm, SE Norway—W Sweden. Sveriges geologiska undersökning, Ser. C No. 817, pp 1–61. Uppsala 1987.

The 1420 Ma old Kattsund-Koster dyke swarm, which comprises the Koster dykes of western Sweden and the Kattsund dykes of southeastern Norway, is a very dense dyke swarm concisting exclusively of tholeiitic dykes. In the Koster archipelago the dyke swarm enters a ductile shear zone in which the swarm became strongly deformed and the dykes recrystallised totally to amphibolites. The Kattsund dykes seen farther to the north are situated within the shear zone.

Detailed chemical investigations on the Kattsund dykes, which are now amphibolites, demonstrate that dykes ≥2 m in width consist of a central zone and two marginal zones. In the central zone the igneous chemistry is well preserved, while the marginal zones, which acted as filters, have normally been enriched in $K_2O$, $H_2O$, Rb, Ba, U, (La), Cl and depleted in $SiO_2$, $TiO_2$, CaO, $Na_2O$, $Fe_2O_3$/FeO and Sr. The thinner dykes (≤2 m) have no central zones.

In the Koster area, where the transition dolerite-metadolerite-amphibolite has been studied, the metamorphic dykes are enriched in $H_2O$, but otherwise no important alteration of the igneous chemistry has taken place except in some of the thinner dykes which have been enriched in $K_2O$ and Rb and depleted in $Na_2O$ and Sr.

Along the axis of the dyke swarm, there were presumably located several open reservoirs at a shallow crustal level (≤15 km). The Kattsund dykes were tapped from one such reservoir, while the Koster dykes were tapped from another. The initial magmas of both the Kattsund dykes and the Koster dykes were ol-tholeiitic types best described as normal (N-type) MORB, selectively contaminated with $K_2O$, Rb and Ba. The Kattsund dyke magma was slightly, but significantly, different to the Koster dyke magma and also became more strongly contaminated. By fractionation of olivine, clinopyroxene and plagioclase the magmas became strongly evolved and enriched in FeO*, $TiO_2$ and incompatible minor and trace elements. The Kattsund dykes show an unusual decrease in $K_2O$ and Rb with increasing fractionation. These trends are explained as the result of mixing between a magma uncontaminated with respect to $K_2O$ and Rb and a magma which early in its history became contaminated with respect to these elements.


## INTRODUCTION

The Proterozoic Kattsund-Koster dyke swarm (Hageskov 1984) is a dense swarm of tholeiitic dykes, which occurs in the Kongsberg-Bamble-Østfold segment of the Sveconorwegian province of the Baltic shield (Fig. 1). The dyke swarm comprises the Kattsund dyke swarm of the Sandbukta-Mølen area within Oslofjorden (Hageskov 1978) and the Koster dyke swarm of the Koster archipelago, Bohuslän (De Geer 1899, 1902, Asklund 1950, Hageskov 1984, 1985). In the Koster area the dyke swarms enters a ductile sinistral shear zone which presumably follows the swarm from Koster to the Sand-

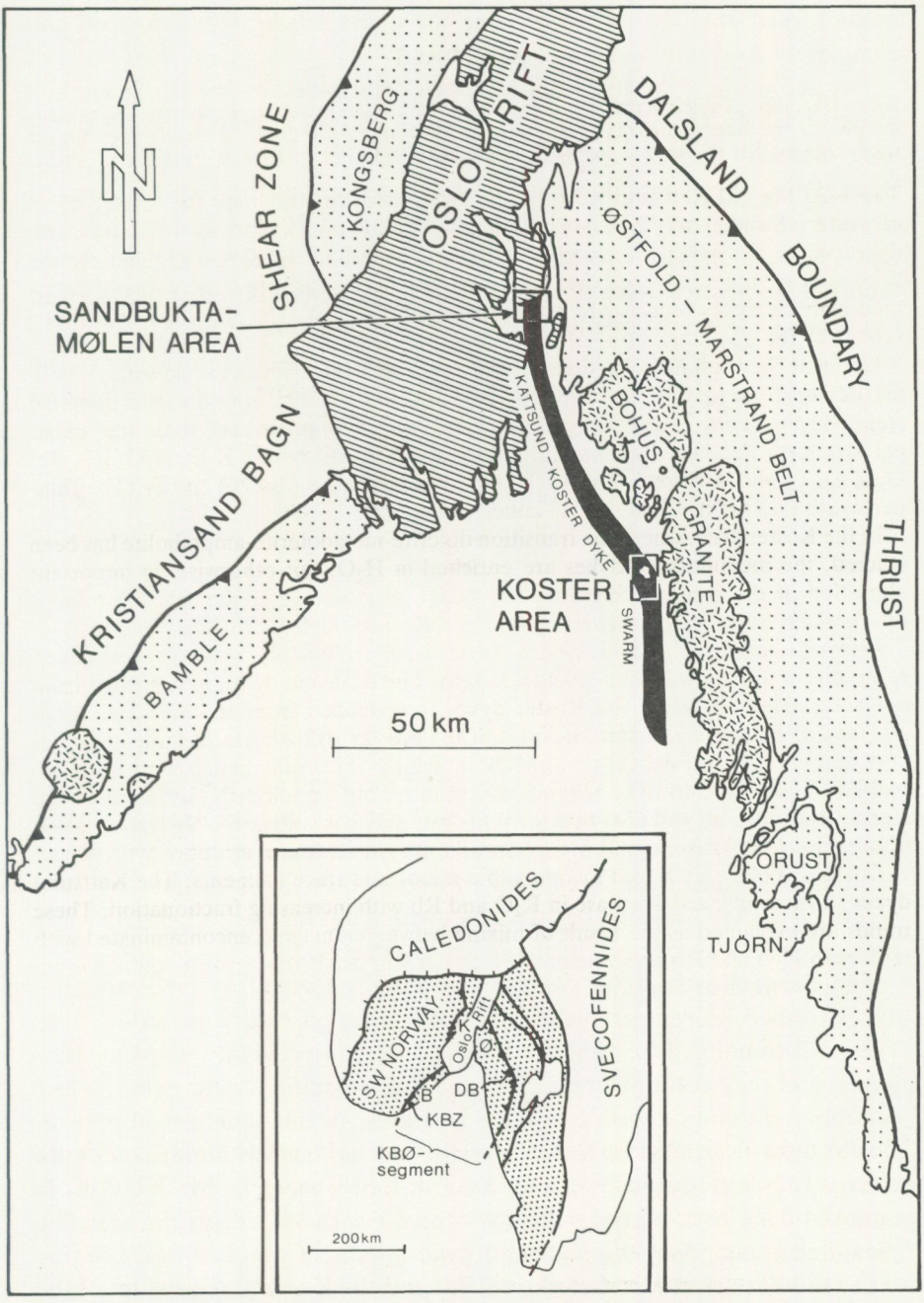


Fig. 1. Sketch map showing the position of the Kattsund-Koster dyke swarm within the Kongsberg-Bamble-Østfold segment (the KBØ segment) of the Sveconorwegian province. Inset map shows the Sveconorwegian province (dotted) and its subdivision into segments by major shear zones.

bukta-Mølen area. In the shear zone the dykes are heavily deformed and completely recrystallised to amphibolites.

The age of the dyke intrusion has been determined by the Rb/Sr method to be 1421 Ma, IR = 0.7028 (Hageskov & Pedersen in prep.) and the dykes are believed to be metamorphosed at 1015 Ma (Hageskov & Pedersen 1981). Basic dykes of possibly the same age are reported from the coastal area of western Sweden and they have been related to the 'Koster diabase dike system' (Asklund 1950) or to 'the Orust dykes' (Daly et al. 1983), which are reported to cover a suite of deformed and metamorphosed dykes seen in Orust and Tjörn in the southern part of Bohuslän. Some of the Koster dykes and the Kattsund dykes are expected to be the probable equivalents of the Orust dykes (Daly et al. 1983). To avoid confusion *'The Kattsund-Koster dyke swarm is the name for the intensely dyked zone running along the coast of Bohuslän and into the Oslofjorden'.*

The aim of this paper is to study and discover the igneous chemistry of the dykes as well as the changes connected to the superimposed metamorphism under the conditions of very high strain.

## THE KOSTER DYKE SWARM

The Koster dyke swarm (Plate 1) occurs in the small and well exposed Koster archipelago in the extreme west of Bohuslän. In that archipelago already De Geer (1899) recognized the occurrence of a dense dyke swarm, which has become transformed to layers of amphibolite. The dykes were later described by Asklund (1950) and reinvestigated by Hageskov (1985), in which previous works and details of the dykes are described.

The dense Koster dyke swarm is essentially formed by NNE trending dykes formed by repreated dyke by dyke injection over a period of time. The NNE trending dykes (the NNE dykes) were injected into simple dilation joints, and they cut a few older NE and NW trending Koster dykes, which possibly were emplaced in conjugate fractures. In the undeformed part the Koster dyke swarm has at least the width of 8 km, and within this width the crust is regularly dyked by about 700 dykes of a mean width of 2.2 m. In total the dyke rock occupies 15—20% of the rock mass, and the crust has expanded about 1500 m across the Koster area by dyking.

In the NE part of the Koster area the dyke swarm is deformed in a steep NW—SE trending ductile shear zone. On the basis of the degree of this amphibolite facies deformation and recrystallisation the Koster area is divided into three sectors (Fig. 2).

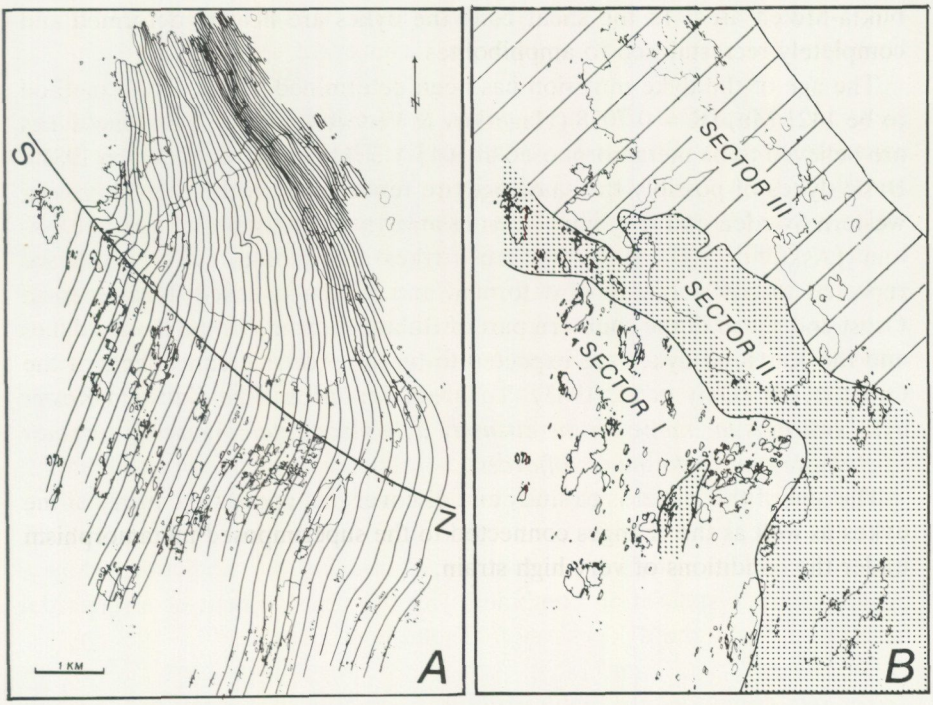


Fig. 2. A) shows the trend of the Koster dyke swarm, which is bent in a shear zone, the SW margin of which is indicated by the line SZ. B) shows the subdivision of the Koster area into sectors (see text).

## DESCRIPTION OF THE DYKES WITHIN THE SECTORS

*Sector I:* The dyke swarm is undeformed and the dykes are very slightly altered. The dykes are mainly aphyric tholeiitic dykes, but about 5% are porphyritic with small (<1 cm) phenocrysts of olivine and/or plagioclase. The dykes show chilled margins against the host gneisses. The typical dyke rock is formed of plagioclase (An 70—35), clinopyroxene, ± olivine, ± hypersthene, hornblende, apatite, zircon, titanomagnetite, ilmenite and ±pyrrhotite. The plagioclase is dusty brown and shows an overall normal zonarity which often is associated with oscillations. It is commonly seen that olivine reacted with plagioclase to form a double corona of hypersthene and pale hornblende, and to varying degree olivine has been replaced by ilmenite-orthophyroxene symplectites. These reactions took presumably place during or immediately after the late magmatic crystallisation as proposed by Zeck et al. (1982). Orthopyroxene in the rocks is only seen due to these reactions. Evidence of post-crystalline deformation is widely seen by straining of the

silicate minerals. Here and there the dykes show signs of incipient amphibolitisation as the result of the amphibolite facies event.

*Sector II:* A transitional zone between the fresh dykes of sector I and the completely recrystallised dykes of sector III. The dyke rocks in sector II are metadolerites with well preserved doleritic texture. The amount of recrystallisation induced by the amphibolite facies event varies strongly from about 15% to nearly 100%. These percentages express the amount of recrystallised grains in relation to the igneous grains + the grains formed by the late magmatic reactions. Thus metadolerites with substantial amounts of igneous mineralogy as well as pure amphibolites occur. When present the primary minerals are often subdivided into smaller grains and amphibole (uralitic hornblende) may be a main constituent. The olivine is replaced by complex aggregates including ilmenite, biotite, hornblende, ± orthopyroxene and ± sphene. Decimeter-wide relic chilled dyke margins are always present, but often they are sheared in a cm-wide zone along the contact. The sheared rock is a biotite-chlorite bearing amphibolite. Thin dykes may sometimes show a prominent recrystallisation combined with the development of a sigmoidal foliation. Locally the dykes show folds and boudinage.

*Sector III:* The dykes are highly strained by ductile stretching, and they are completely recrystallised to amphibolites, which show a pronounced lineation defined by minerals (hornblende) and aggregates (plagioclase). Only a few wide dykes have preserved a relic doleritic texture in their centres. In spite of the recrystallisation mimetic chilled margins can be seen. A less pronounced foliation may be seen together with the lineation. Synkinematic garnets have locally been formed, and they overgrow the lineation. The amphibolites themselves consist essentially of hornblende, plagioclase (An 35—25) and a minor amount of biotite which is more or less replaced by chlorite. No titanomagnetite occurs, but fresh ilmenite is seen in some dykes, while in others it is altered to sphene.

## THE KATTSUND DYKES

The Kattsund dykes form a dense swarm of completely amphibolised dykes which have been exposed also to a very strong deformation resulting in a pronounced stretching. In the present deformed stage the Kattsund swarm consists of at least 600 parallel and steeply inclined dykes and major dyke branches in an area only 2.5 km across. Some multiple dykes are found in the form of a younger dyke within an older of approximately the same chemi-

cal composition. Generally the dykes are <2.0 m wide and only a few reach 10 m in width. About 1/3 of the total rock mass is made up by the dykes. The contacts between the dykes and the gneiss are sharp and no reaction zones related to the dyke injection or to the later metamorphism are visible. The superimposed ductile deformation has thinned the dykes as well as the gneiss layers, but the ratio between the amount of dyke rock and the amount of gneiss is presumably close to the original dyke/gneiss ratio, because of a bulk homogeneous deformation. In the Koster archipelago this deformation is demonstrated to have no influence on the original dyke/gneiss ratio (Hageskov 1985).

## PETROGRAPHY

In the dykes nearly all primary textural relations have been destroyed and no primary silicate minerals are present. The dyke rock appears now as a fine grained strongly lineated and slightly foliated amphibolite. Oblate cigar-shaped plagioclase aggregates define both the lineation and the foliation. Hornblende nematoblasts parallel the lineation. In the central part of the dykes the plagioclase aggregates are usually 2—3 cm long and about 1—2 mm across, but their dimensions as well as the dimensions of the hornblende nematoblasts decrease towards the dyke margins. The dyke margins themselves are sheared and foliated parallel to the contacts.

The decrease in textural size towards the margins undoubtedly reflects an original chilling and palimpsest (mimetic) chills (Fig. 3) are seen along the interior margins of the multiple dykes.

The central parts of the dykes, including internal chilled margins, are essentially composed of hornblende (62—69%), plagioclase (18—29%), quartz (2—9%), biotite + chlorite (<5%) and opaque + sphene (3—6%). As accessories apatite and zircon occur. The plagioclase is moderately altered and has an An content of 27—32%, sometimes with an irregular core of An 23%. The plagioclase with An 27—32% centres may show a slight normal zonality to An 22—25% at the margin. The biotite shows alteration to chlorite + sphene + alkali-feldspar, otherwise no alkali-feldspar is observed. The hornblende is fresh. Sphene varies in amount and is commonly associated with the ilmenite.

The fabric and the mineralogical composition of the dyke margins show a rather wide variation from slightly sheared and foliated amphibolites to strongly sheared biotite-amphibole schists in which the biotite in varying degree is replaced by chlorite. In the less altered margins the mineralogical composition is close to that seen in the dyke centres, but the biotite (+ chlorite) content exceeds 10% and more sphene is formed at the expenses of the Fe-Ti oxides.

Fig. 3. Internal palimpsest chilled margin of a multiple Kattsund dyke.

The more sheared margins have a larger amount of biotite (+ chlorite) and quartz, and the hornblende becomes light green. In the most extreme margins the mica content reaches 35% and some albite occurs. Two generations of biotite are seen; an older generation defining the foliation and deformed by kinks, and a younger generation growing across these structures. The chlorite replacement is younger than the second biotite generation. No alkali-feldspar occurs and epidote and muscovite are rare.

## THE SANDBUKTA GNEISS

The host rock to the Kattsund dykes is the very fine grained and homogeneous Sandbukta gneiss. This leucocratic granitic rock is believed to represent a gneissified intrusive quartz-feldspar porphyry (Hageskov & Pedersen 1981) which was very uniform in chemical composition prior to the superimposed metamorphic event (see Table I). Samples collected at a distance of more than 1 m from the nearest dyke demonstrate the small chemical variation. The chemical uniformity, the small grain size and the strong chemical contrast to the Kattsund dykes make the Sandbukta gneiss attractive for a study of metasomatic element exchange between basic and granitic rocks.

## GEOCHEMISTRY

In the Koster area only the fresh dykes of sector I can be treated as igneous rocks, and when it has not been possible with certainty to follow single dykes from sector I to sector III, the chemical alterations have to be discovered by comparing the altered dykes to the magmatic trends shown by the fresh sector I dykes. As the transformation of fresh dolerite to heavily deformed amphibolite of sector III took place over less than 3 km, it is expected, that within this short distance no primary chemical differences should have existed between the mean dykes of sector I, II and III.

In the Kattsund dyke swarm the primary chemistry of the magmatic rocks has to be deduced from the amphibolites themselves. Metasomatic changes of the Kattsund dykes can not be demonstrated by comparing these dykes to the fresh Koster dykes, because although they presumably were injected contemporaneously there may well exist a primary difference between the two dyke swarms. The analytical methods are described in Appendix, p. 43.

### SAMPLING OF THE DYKES

To study the igneous chemistry of the Kattsund dykes, profiles were densely sampled across three multiple dykes. From that investigation discussed later on it is obvious that dykes thicker than 2 m consist of a *central zone,* in which the element variation is small, regular and approximately symmetric, and two *marginal zones,* showing increasing chemical changes towards the contacts. The study of the profiles suggests that the primary igneous chemistry is well preserved in the central zone, while the variation seen in the marginal zones presumably is related to metasomatism, but effects from selective contamination and magmatic differentiation may also be involved in the variation. Thin dykes have no central zones; only two adjoining/overlapping marginal zones. This information about the chemical pattern within the dykes has guided the method of sampling of both the Koster dykes and the Kattsund dykes.

In the Kattsund dyke swarm 16 samples have been collected in the centres of dykes >2.5 m wide to be well inside the central zone. These samples have been taken to test if the primary chemistry is well preserved and to discover aspects of the petrological evolution of the dyke swarm. In the Kattsund dyke swarm also paired samples were collected. Each pair consists of one sample from the dyke margin and one sample from the central zone of the same dyke >2.5 m. The paired samples were collected to study the marginal zones and are thus supplementary to the profiles. These paired samples are called M-pairs.

Besides the M-pairs, I-pairs and G-pairs have been collected. The I-pairs are paired samples taken in the centre and the margin (palimpsest chill) of younger interior dykes within multiple Kattsund dykes. These also amphibolised interior dykes have been protected by the shells of the older dyke and may give information about the pre-metamorphic differences between dyke centre and dyke margin. The G-pairs are taken in the homogeneous host gneiss to the Kattsund dykes and a G-pair consists of one sample taken close to a dyke contact (marginal sample) and one sample taken more than one meter from a dyke contact (centre sample) in the same gneiss layer between two Kattsund dykes. The idea of the G-pairs is to get information about element exchange between dyke and gneiss "layers".

In the Koster area 18 samples have been collected from the centres of the fresh dykes of sector I, and 12 samples from the centre of sector II metadolerites. In the high strain belt of sector III there have been collected 13 samples in the centre of dykes >2 m and 10 samples of dykes <2 m. The samples from sector I were collected for the study of the igneous petrology, while the samples from sector II and III were collected for the study of metasomatic alterations with respect to the sector I dykes. In the high strain belt four paired samples of the M-type have been collected.

## THE PRE-METAMORPHIC CHEMISTRY OF THE DYKE SWARMS

### SAMPLES FROM THE DYKE CENTRES

The samples discussed are from the centres of Koster dykes from sector I and from the central zone of Kattsund dykes ≥2.5 m. To test whether the primary chemistry is well preserved in the central zone of the Kattsund dykes and to discover the primary chemical variation the analytical results (Table II and III) are plotted in various binary and ternary diagrams. The analyses given are all from aphyric or originally aphyric dykes.

The samples from the two dyke swarms show that they both basically consist of olivine tholeiites (in the sense of Yoder & Tilley 1962), but they include also highly evolved, just quartz tholeiitic dyke member (Fig. 4A). The normative Ol,Py,Pl diagram (Fig. 4B) shows that the Koster dykes as well as the Kattsund dykes follow the distribution of MORB samples from DSPD and the Famous area on the Mid-Atlantic ridge (Bryan *et al.* 1976).

In the variation diagrams (Figs. 5, 6), where FeO*/MgO is used as differentiation index (Miashiro 1973), all elements show rather well defined trends. The trends are typical of tholeiites except for the $K_2O$, Rb and Ba trends of the Kattsund dykes. The contents of $K_20$, Rb and (Ba) decrease with increasing FeO*/MgO, which is unusual in tholeiitic series.

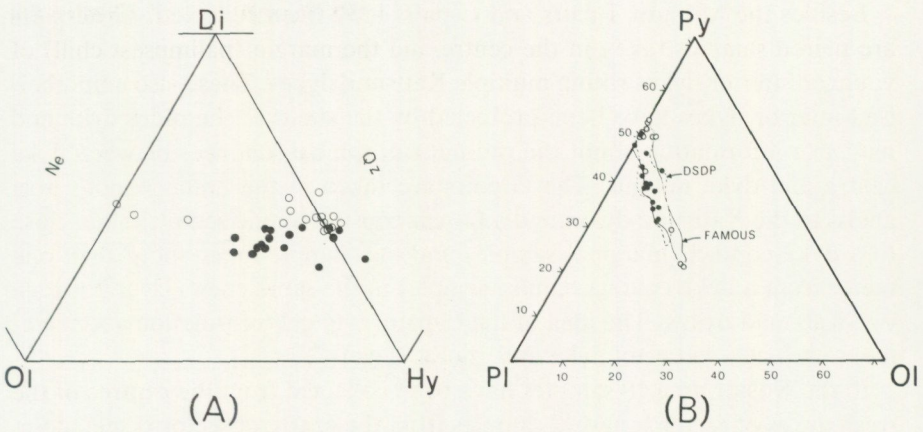


Fig. 4. A) Variation in the normative olivine, diopside and hypersthene composition of the Koster and Kattsund dykes. B) Variation in the normative plagioclase, pyroxene and olivine composition of the Koster and the Kattsund dykes. Circles = Kattsund dykes. Filled circles = Koster dykes of sector I.

Both dyke swarms include highly evolved dyke members. The FeO*/MgO ratio varies from 1.32 to 4.32 in the Koster dyke swarm when well preserved samples from sector II are included. In the Kattsund dyke swarm the FeO*/MgO ratio varies from 1.36 to 3.26. The trends shown by the two dyke swarms (except for $K_2O$, Rb, Ba of the Kattsund dykes) are closely related, but there are differences in the levels of the element contents. The contents of $Al_2O_3$, $TiO_2$, CaO, $P_2O_5$, La, U, Y, Zr, Nb, Ni and Cr are higher in the Koster dykes, while the contents of $SiO_2$ and V are lower. These differences may indicate that the Kattsund dyke magma was derived from a mantle source more depleted/melted than the source of the Koster dyke magma.

It is characteristic in both dyke swarms that: 1) $SiO_2$ and $Na_2O$ are almost constant, 2) CaO and Sr decrease slightly with increasing FeO*/MgO, 3) the evolved dyke members become strongly enriched in FeO* ($\geq$16%), $TiO_2$ ($\geq$3%) and incompatible trace elements. Enrichment in FeO* and $TiO_2$ with increasing FeO*/MgO and almost constant $SiO_2$ level are typical features of the oceanic tholeiites (Miashiro 1973). Strong FeO* and moderately strong $TiO_2$ enrichment are a.o. shown in basalts from Galapagos (Clargue & Bunch 1976, Byerly et al. 1976) and in the Skaergaard intrusion, which also has affinity to the MORB type (Brooks & Nielsen 1978).

In the AFM diagram (Fig. 7) the Koster dyke swarm closely follows the trend of the Skaergaard liquid, but apparently the most evolved Koster dykes became more enriched in alkalies. The Kattsund dyke swarm shows a well defined, but unusual trend, with decreasing amounts of alkalies ($K_2O$) with increasing amount of FeO*.

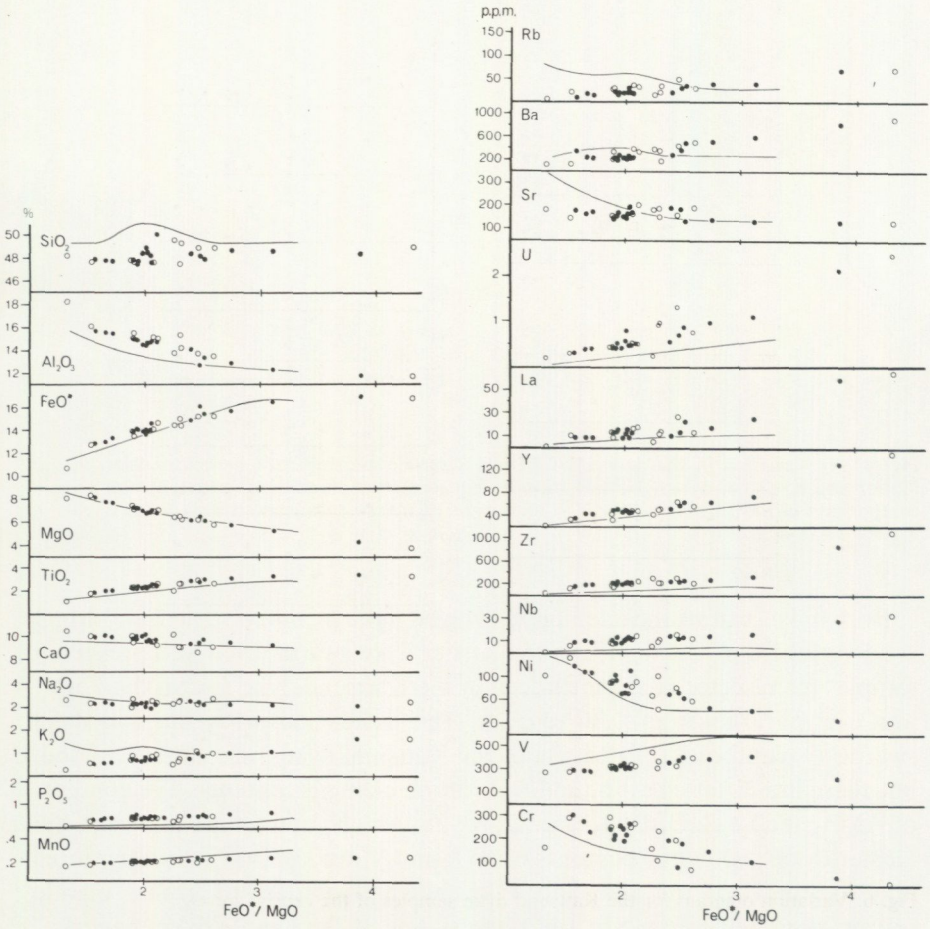


Fig. 5. Variation diagrams for the Koster dykes. Circles = Koster dykes of sector II, filled circles = Koster dykes of sector I. The lines shown are the trend lines of the Kattsund dykes (Fig. 6).

Even though $K_2O$ is high in the less evolved Kattsund dykes, the total amount of alkalies are within the limits of the tholeiites (Fig. 8). Also the Koster dykes plot in the field of tholeiites in the $SiO_2$ versus $Na_2O + K_2O$ diagram.

Plotting $CaO/TiO_2$ and $Al_2O_3/TiO_2$ against $TiO_2$ in the diagrams of Sun and Nesbitt (1978), decreasing evolution trends are seen within and continuing the field of MORB (Fig. 9). The most primitive sample of the Koster dykes (LS 7) plots above the MORB field in the $Al_2O_3/TiO_2$ diagram. However this sample is supposed to represent a residuum of a magma from which olivine and chromite have been fractionated.

La, U, Zr, Rb, Ba, Nb and Y behaved as incompatible elements during

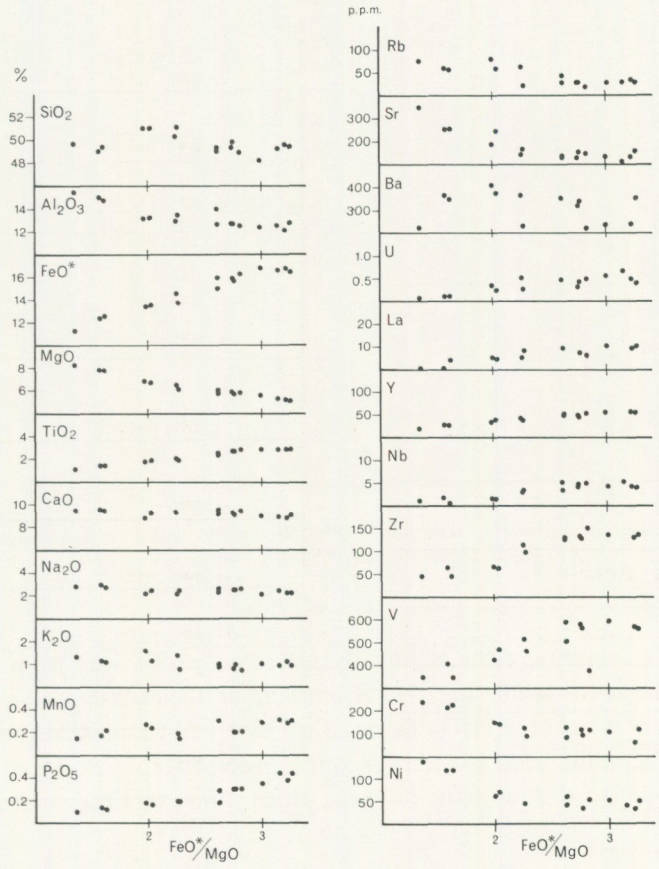


Fig. 6. Variation diagram for the Kattsund dyke samples of the central zones.

the evolution of the Koster dyke magmas and in the most evolved samples (41153, sector II) these elements have been enriched about 13, 12, 11, 10, 9, 7 and 5 times respectively. From the diagrams (Fig. 5 and 6) it appears that the Koster dykes generally are richer in Zr, Nb and Y and slightly richer in $TiO_2$. The differences between the content of these elements are also seen in the ternary (Zr, $TiO_2$, Y) diagram Fig. 10 of Pearce and Cann (1973). The Kattsund dykes plot in the field of low potassium tholeiites and ocean floor basalts, while most of the Koster dykes plot on the boundary between the fields of ocean floor basalts and calc alkali basalts. In both dyke swarms increasing evolution of the magmas results in a movement of the composition towards the Zr apex. Immediately the dykes should be expected to plot in the field of within plate basalts, but many basaltic rocks from continental areas fail to plot in that field (Holm 1982, Zeck & Morthorst 1982).

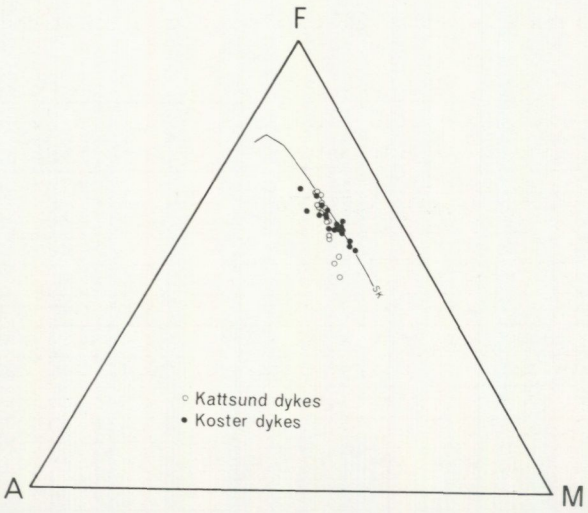


Fig. 7. AFM diagram showing the variation of the Kattsund dykes and the Koster dykes of sector I. The Sk-trend refers to the Skaergaard liquid (Wager 1960).

The $H_2O$ contents of the Koster dykes from sector I vary from 0.44% to 1.42%. The distribution (Fig. 11) is bimodal and shows that a small group of four dykes is richer in $H_2O$. These dykes have been exposed to some alteration. The amphibolised Koster dykes from sector III are enriched by about 1% $H_2O$ relative to the sector I dykes, which shows that the metamorphism

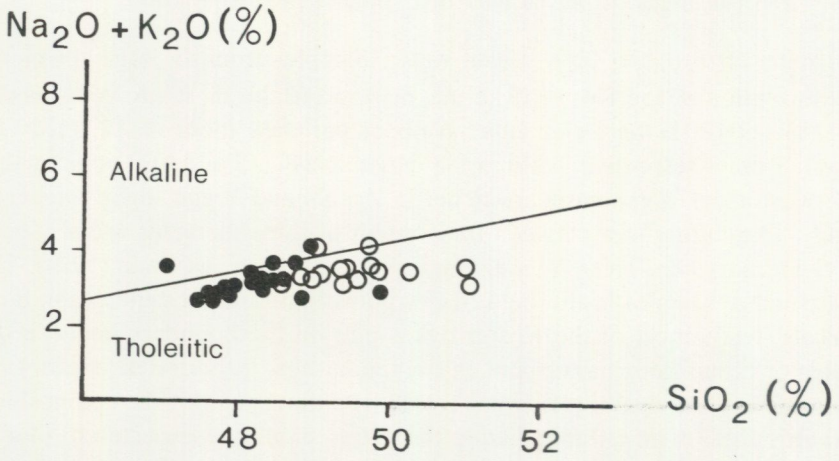


Fig. 8. Plot of total alkalis against silica. The subdivision of the diagram into the fields of alkaline and tholeiitic basalts is based on MacDonald and Katsura (1964). Signatures as in Fig. 7.

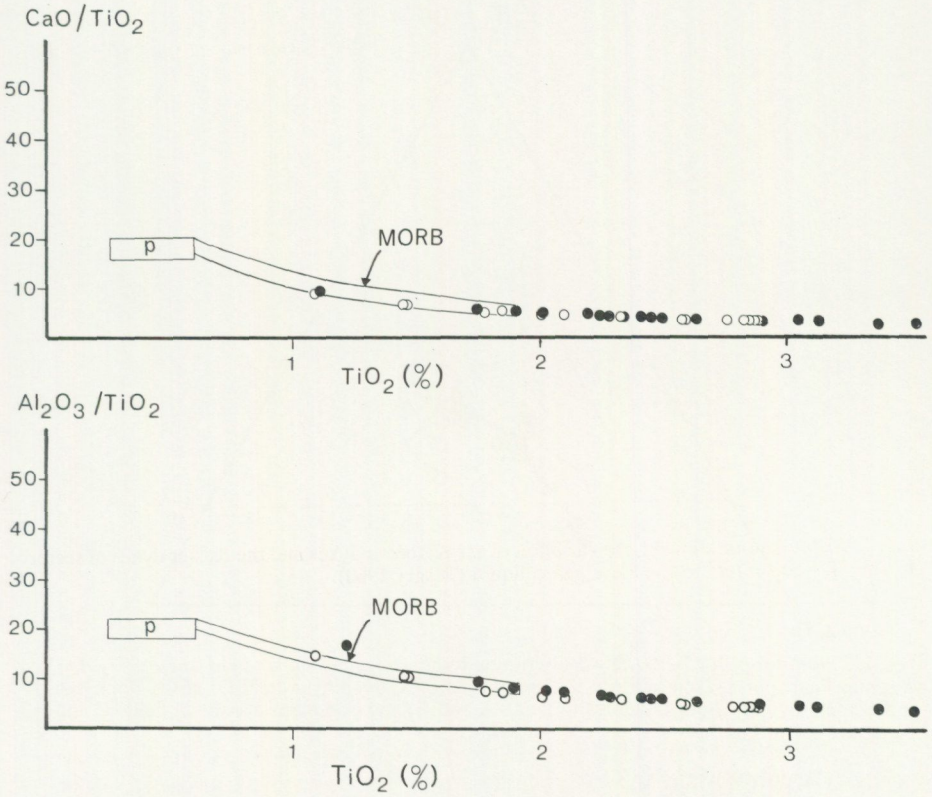


Fig. 9. Plot of $CaO/TiO_2$ and $Al_2O_3/TiO_2$ *versus* $TiO_2$. The fields of MORB and primordial mantle (P) are given by Sun and Nesbitt (1978). Signatures as in Fig. 7.

was accompanied by an influx of water. Samples from the central zones of the Kattsund dykes show a $H_2O$ variation between 0.58% and 2.15% with a mean content of 1.48%. The amphibolitisation of the Kattsund dykes has also been accompanied by an $H_2O$ enrichment.

## PRIMARY (?) CHEMICAL VARIATION BETWEEN CHILLED MARGIN AND DYKE CENTRE

Knowledge of the pre-metamorphic element variation between dyke centre and dyke margin has been obtained from a geochemical profile across a fresh Koster dyke and from three protected slightly younger dykes within the central zone of multiple Kattsund dykes.

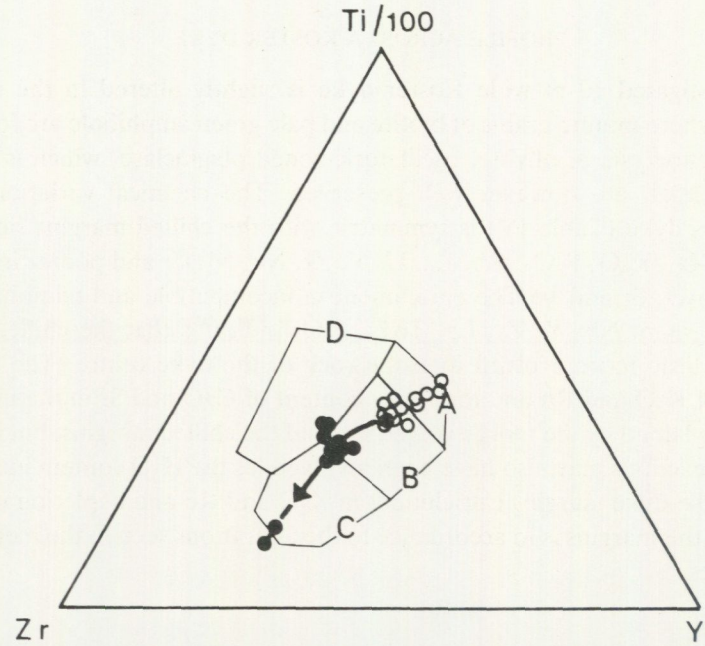


Fig. 10. Plot in the Zr, Ti/100, Y×3 discrimination diagram of Pearce and Cann (1973). In this diagram Pearce and Cann indicate that within plate basalts plot in field D, ocean-floor basalts in field B, low-potassium tholeiites in fields A and B, and calc-alkali basalts in fields C and B. Signatures as in Fig. 7.

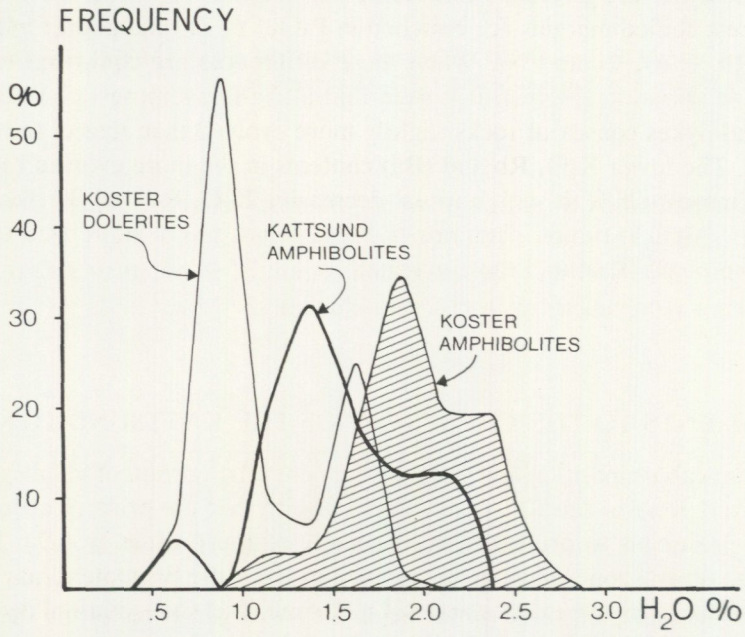


Fig. 11. $H_2O$ content in the Koster dolerites, Koster amphibolites and the Kattsund amphibolites.

### PROFILE ACROSS A KOSTER DYKE

The investigated 10 m wide Koster dyke is slightly altered in the chilled margins where minute grains of biotite and pale green amphibole are formed. Small phenocrysts of olivine, oscillatoric-zoned plagioclase, which is sometimes skeletal, are however well preserved. The chemical variation seen across this dyke (Table IV) is symmetric with the chilled margins richer in $TiO_2$, $Al_2O_3$, $K_2O$, $P_2O_5$, Rb, La, U, Y, Zr, Nb, Ni, Cr and poorer in CaO, FeO*, $Na_2O$, Sr and V. The enrichment in incompatible and immobile/less mobile element Nb, Y, Zr, La, $TiO_2$, $P_2O_5$ indicates that the chilled dyke rock is a little more evolved than the rock of the dyke centre. The higher content of $K_2O$ and Rb and the lower content of CaO and Sr in the margins can be explained by the more evolved stage of the chilled margins, but hydrothermal reactions may also have been involved, as the $H_2O$ content increases towards the dyke margin. Enrichment in $K_2O$ and Rb and depletion in CaO and Sr in the margins is in accordance to the alterations seen in the metamorphic dykes.

### THE PROTECTED KATTSUND DYKES

Chemical analyses of I-pairs collected in protected dykes within multiple Kattsund dykes are given in Table XII. From the analyses it appears that the palimpsest chilled margins are enriched in $P_2O_5$, Y, Zr, and poorer in $K_2O$, CaO, Rb, (Ba), Cr and Ni. When these differences are compared to the magmatic variation (Fig. 6), it is seen that also the palimpsest chills of the Kattsund dykes consist of rocks slightly more evolved than that of the dyke centres. The lower $K_2O$, Rb and (Ba) contents in the more evolved rock of the palimpsest chills fit with unusual decreasing $K_2O$, Rb and Ba trends in the FeO*/MgO variation diagrams, if these trends are to be related to the evolution of the Kattsund dyke magma.

## COMMENTS TO THE CHEMISTRY OF THE KATTSUND DYKES

The chemical composition and the inter-element relationships of samples from the central zone of the Kattsund dykes indicate that the primary chemistry is well preserved as predicted by the study of the profiles (p. 27). However, the central zones have been enriched in $H_2O$, the Ba content may have been disturbed in some dykes and $K_2O$, Rb and (Ba) show unusual decreasing trends with increasing evolution of the dyke magma.

These decreasing trends can be explained in two ways: 1) $K_2O$, Rb and Ba have been metasomatically enriched in some of the central zones and by accident the less evolved samples came from enriched central zones, 2) The observed trends are related to the magmatic history of the dykes. Suggestion 1) is favoured by the high mobility of these elements which have migrated inwards and enriched the marginal zones of the dykes (p. 34), but 1) is unacceptable because the interior protected dykes show lower and not higher contents of $K_2O$, Rb and Ba in their palimpsest chilled margins than in their centres. The lower content of $K_2O$, Rb and Ba in these margins fit as mentioned with the more evolved stage of the chilled dyke rock and argues for a $K_2O$, Rb and Ba variation related to the magmatic history of the dykes.

## THE EVOLUTION OF THE KOSTER AND THE KATTSUND DYKE MAGMAS

The geochemically most primitive Koster dyke is found in a well preserved sample from sector II (sample LS 7). That dyke has been enriched in $H_2O$, but apparently there is no enrichment/depletion in mobile elements such as $K_2O$, Rb and Ba when this dyke is compared to the evolution trends of the Koster dyke magma. The low contents of MgO, Cr and Ni suggest that the sample represents a magma in which olivine and chromite have been fractionated. Judged from the trends, values of MgO ~ 9%, Ni ~ 160 ppm and Cr ~ 400 ppm appear to be the original values of this magma. In Fig. 12 this sample is given as the "primitive Koster magma" while a mean of the three least evolved Kattsund dyke samples is given as "the primitive Kattsund dyke magma". In Fig. 12 these compositions are compared to analyses of MORB, island arc tholeiite, Galapagos ferrobasalt and some olivine tholeiites from continental environments.

Compared to the basalts in this table, it is apparent that both the Koster and the Kattsund dyke magmas are high/very high in $K_2O$, Rb and Ba. Disregarding these elements which presumably have been enriched by selective crustal contamination, both the Koster and the Kattsund dyke magmas are related to the present MORB and the almost similar island arc tholeiite as demonstrated by the low content of incompatible elements (U, Th, Y, Nb, Zr). The two dyke magmas show by their higher $TiO_2$, Cr and Ni content a closer agreement with the MORB type than to the island arc tholeiite. The Zr/Nb, Zr/Y and Y/Nb ratios (see Fig. 13) suggest the dyke magmas to be of the N type of MORB (Le Roex et al. 1985). The Kattsund and Koster dyke magmas can then be described as N-MORB type tholeiites enriched in $K_2O$, Rb and Ba.

| | 1 | 2 | 3 | 4 | 5 | 6 | 7 | 8 |
|---|---|---|---|---|---|---|---|---|
| $SiO_2$ | 48.16 | 49.39 | 50.67 | 51.57 | 48.54 | 47.69 | 48.6 | 50.27 |
| $TiO_2$ | 1.11 | 1.33 | 1.28 | 0.80 | 1.77 | 2.35 | 1.22 | 1.58 |
| $Al_2O_3$ | 18.16 | 15.10 | 15.45 | 15.91 | 14.83 | 14.81 | 13.7 | 15.52 |
| MgO | 8.03 | 7.95 | 8.05 | 6.73 | 7.51 | 8.65 | 7.42 | 6.65 |
| CaO | 10.53 | 9.50 | 11.72 | 11.74 | 11.81 | 10.00 | 11.9 | 12.28 |
| $Na_2O$ | 2.61 | 2.86 | 2.51 | 2.41 | 2.33 | 2.66 | 2.06 | 3.13 |
| $K_2O$ | 0.30 | 1.18 | 0.15 | 0.44 | 0.31 | 0.73 | 0.33 | 0.23 |
| $P_2O_5$ | 0.10 | 0.12 | - | - | 0.19 | 0.19 | - | 0.11 |
| FeO* | 10.63 | 12.09 | 9.67 | 9.51 | 11.05 | 12.22 | 11.7 | 10.10 |
| FeO*/MgO | 1.32 | 1.52 | 1.20 | 1.41 | 1.47 | 1.41 | 1.58 | 1.52 |

| | | | | | | | | |
|---|---|---|---|---|---|---|---|---|
| Rb | 7.5 | 65 | 1 | 5 | 11.6 | | 10 | |
| Ba | 126 | 316 | 12 | 75 | 22 | | 80 | |
| Sr | 182 | 287 | 123 | 200 | 245 | | 145 | |
| La | <2 | 1.5 | 4.7 | 1.1 | | | | |
| Y | 22 | 26 | 33 | | | | 25 | |
| U | 0.190 | 0.109 | 0.10 | 0.15 | 0.259 | | | |
| Th | <1 | <1 | 0.18 | 0.5 | | | | |
| Zr | 62 | 50 | 100 | 50 | 127 | | 82 | |
| Nb | 1.2 | 1.3 | 3.1 | 2 | | | | |
| Ni | 99 (160) | 125 | 123 | 30 | 110 | | 84 | |
| V | 263 | 366 | 289 | 270 | 272 | | 315 | |
| Cr | 156 (400) | 228 | 296 | 50 | 252 | | 256 | |

Fig. 12. Showing the compositions of: 1) The primitive Koster dyke magma, 2) the primitive Kattsund dyke magma, 3) MORB, major elements from Bryan *et al.* (1976), table 2,2, trace elements from Sun and Nesbitt (1977) and Coleman (1977), 4) Island arc tholeiite, Jakes and White (1972), 5) FG — 1 dyke generation, dyke B, Brooks and Nielsen (1978), 6) Lava from Snake River Plain, Stout and Nicholls (1976), Table 9 group 1 non-porphyritic, calculated avg. free of $H_2O$, 7) Southern Tobacco Root Mountain dykes, Wooden et al. (1978), Table i, group A, 8) Differentiated MORB, Galapagos Spreading Centre, Claugue and Bunch (1976), Table 1, differentiate 1.

| | KOSTER DYKES | KATTSUND DYKES | N-MORB | |
|---|---|---|---|---|
| | | | American Antarctic Ridge | Southwest Indian Ridge |
| Zr/Nb | 17-52 | 21-72 | 17-78 | 17-64 |
| Zr/Y | 2.8-4.8 | 1.8-2.9 | 2.2-4.2 | 1.8-3.6 |
| Y/Nb | 3.5-18.3 | 7.9-46.7 | 4.6-23 | 8-22 |

Fig. 13. Zr/Nb, Zr/Y and Y/Nb ratios of Koster dykes, Kattsund dykes and normal (N) MORB. (Values from Le Roex *et al.* 1985).

The evolution trends of the Koster and the Kattsund dyke magmas are satisfied by fractionation of Pl, Cpx and Ol in the ratio of 3.6 : 1 : 1.6 in the case of the Koster dykes, while the figures for the Kattsund are 4.4 : 2.5 : 1. The evolution of the dyke magmas from olivine tholeiitic parent magmas to quartz normative tholeiites suggests fractionation at a shallow level $\leq$5 Kbar (15 km) (Green & Ringwood 1967).

The Kattsund dykes and the Koster dykes can not have been drawn from the same magma reservoir because of the differences between the magmas. Most likely several magma reservoirs have been located along the axis of the dyke swarm. The Koster and the Kattsund dykes could each have been drawn from such larger reservoirs situated at shallow levels below the dyke swarms (Fig. 14). If so, the magma reservoirs must have been refilled. In the Koster dyke swarm four successive NNE dykes have been analysed and they (41125, 41124, 41127, 41128) show the following FeO*/MgO ratios and (Zr) contents given with decreasing age: 3.12 (326), 1.94 (240), 1.90 (144) and 3.86 (850). This dyke sequence has not been drawn from a fractionating magma in a closed reservoir. In three other cases the chemistry of older and younger dykes has been investigated, but in these cases the older dykes were the less evolved. In the Kattsund dyke swarm the study of the multiple dykes demonstrated that the younger dyke in one of four cases is more evolved than the older dyke.

The low contents of U, Th and La as well as the Zr/Nb, Zr/Y and Y/Nb ratios in the primitive Koster and Kattsund magmas suggest that these magmas have been formed by partial melting of a depleted mantle. Magma produced from such a source would however have given rise to melts with low content of $K_2O$, Rb and Ba. The high contents of these elements in the magmas suggest then that the magmas have been exposed to selective contamination by addition of $K_2O$, Rb and Ba presumably mainly from the crust.

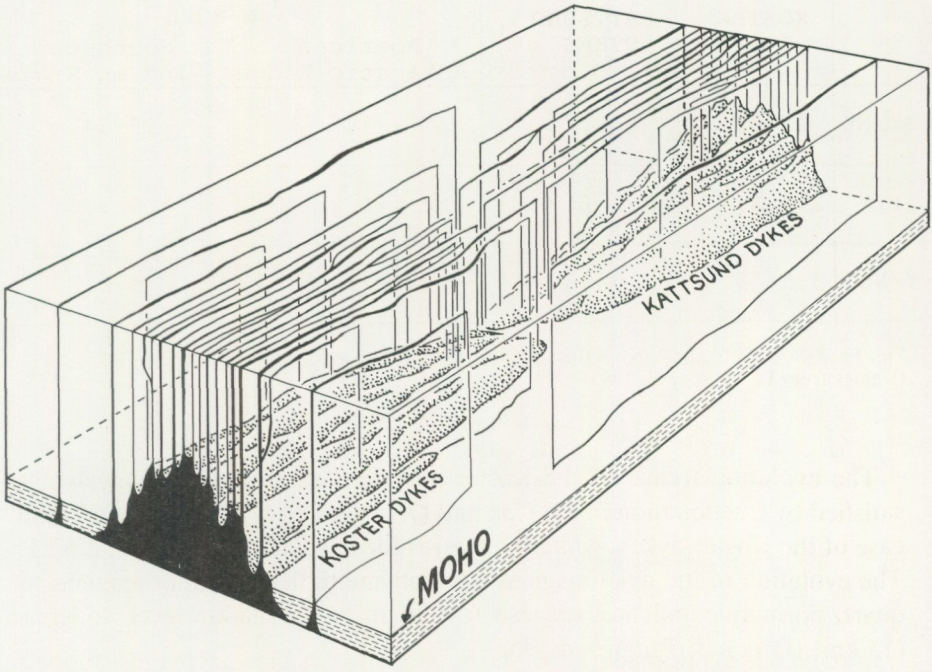


Fig. 14. Sketch showing the Kattsund-Koster dyke swarm. The Kattsund dykes and the Koster dykes have been tapped from separate reservoirs.

The higher concentrations of $K_2O$, Rb and Ba in the primitive Kattsund dyke magma suggest that this magma has been stronger contaminated than the Koster dyke magma, and perhaps that is the main reason for the decreasing evolution trends of $K_2O$, Rb and (Ba) in the Kattsund dyke swarm. These trends can be explained by the following model (Fig. 15).

In stage A a reservoir develops in the continental crust by ascending batches of Ol-tholeiitic magmas. The magma in the developing reservoir becomes selectively contaminated with $K_2O$, Rb and Ba along the crust/reservoir interface. Early dykes have been injected at this stage.

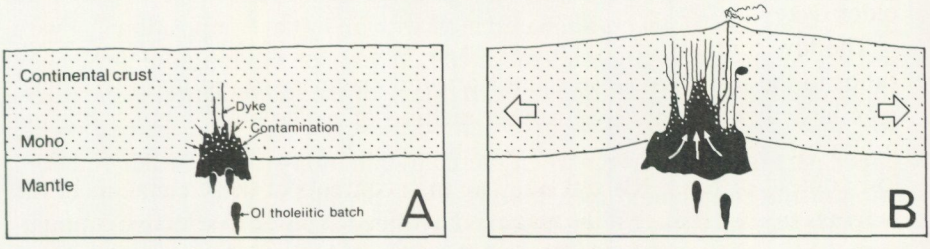


Fig. 15. Model showing the evolution of the Kattsund dyke swarm (see text for explanation).

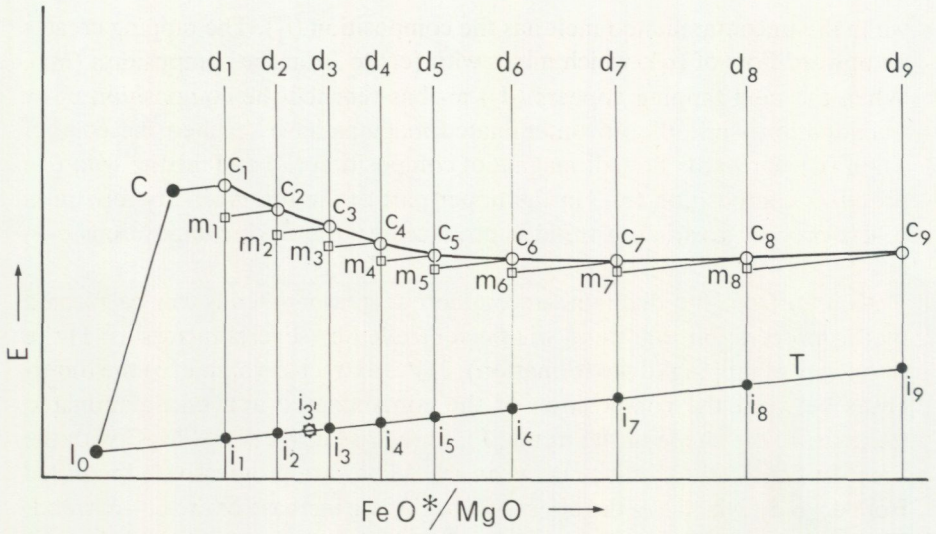


Fig. 16. Model variation diagram (see text for explanation).

In stage B the contamination of the fractionating magma has mainly stopped because of the cooling in the marginal part of the reservoir and because an aureole around the reservoir may have been depleted with respect to the extracted elements. The marginal and the upper part of the reservoir will have been most strongly contaminated if the magma is not well stirred. Tensional forces in the crust then opened joints into which magma from the reservoir was injected. Tapping from the upper part of the reservoir creates an upward flow of less or uncontaminated magma. The upwards flowing magma mixes with the contaminated magma and dilutes the concentration of the contaminants in the upper part of the reservoir. The periodical tapping and upward flow of less or uncontaminated magma continue during the dyke swarm formation.

The mechanism of tapping and mixing is tentatively inspected in the variation diagram Fig. 16. Firstly the process is considered to take place in a closed reservoir. In the variation diagram a simplified trend T is produced by fractionation of uncontaminated melt with an initial composition ($I_o$) with respect to an incompatible element (E). A part of the initial melt became contaminated with (E) during the early stage of the fractionation in the reservoir and a contaminated melt of composition (C) has been formed in the upper part of the reservoir when the contamination stops. Further fractionation of the contamined melt follows a line parallel to (T).

When the first dykes ($d_1$) are formed by tapping of the upper contaminated part of the reservoir the contaminated melt has the composition ($c_1$)

while the uncontaminated melt has the composition ($i_1$). The tapping creates an upward flow of ($i_1$), which mixes with ($c_1$) to form the composition ($m_1$). When the next tapping appears ($d_2$) $m_1$ has reached the composition $c_2$ by fractionation while the uncontaminated magmas have reached the composition ($i_2$). Upwards flow of magma of composition ($i_2$) and mixing with ($c_2$) produces composition ($m_2$) in the upper part of the reservoir. By repetition of the process a variation trend is produced by the dyke compositions $c_1$—$c_2$---$c_9$.

As seen from the diagram, uncommon decreasing trends can be formed by this process, but the trend will be controlled by several factors as: 1) the frequency of tapping (dyke formation), 2) the extracted volume, 3) the differences between the composition of the contaminated and uncontaminated magmas, 4) the shape of the trend (T), 5) the rise of the FeO*/MgO with the time. In Fig. 16 the distance between the d-lines are progressively increased from $d_5$ to $d_9$, which has the effect of a beginning increase of the $c_5$—$c_9$ trend. This increasing distance between the d-lines is here considered to show a) the effect of decreasing frequency of dyke formation and b) the influence of increasing rise in the FeO*/MgO with time. In the latter case the distance between the d-lines represents one and the same time unit.

In an open reservoir where magma batches now and then add uncontaminated magma of a composition about ($I_o$) the same model can be used. Addition of less evolved magma will increase the slope of the $c_1\ c_2 \ldots c_N$ trend as can be seen from the following example. Just before drawing ($d_3$) the composition of the contaminated melt is ($c_3$) while the uncontaminated melt has the composition ($i_3$). Introduction of a new magma batch will move ($i_3$) to the left in the diagram to ($i_{31}$). When the tapping ($d_3$) occurs composition ($c_3$) will mix with the upwards flowing ($i_{31}$) and form a new mixed composition to the left of ($m_3$).

The arguments above indicate that unusual negative sloping trends shown by incompatible elements initially enriched in the reservoir by contamination will be favoured by a situation where 1) the extraxted volumes are of importance to the total volume of the reservoir, 2) the reservoir is open and receives batches of less fractionated and uncontaminated magma, 3) the reservoir is frequently tapped as by dyke by dyke injection.

## CHEMICAL DIFFERENCES BETWEEN KOSTER DYKES FROM SECTOR I, II AND III

The chemical change of the metamorphosed Koster dykes is studied by: 1) comparing mean chemical composition of dykes from sector II and III with

the mean chemical composition of the sector I dykes, 2) comparing the individual samples with the magmatic trends shown by the sector I samples, 3) comparing the chemistry of dyke margin to dyke centre (this study is given together with the study of the M-pairs of the Kattsund dykes). The samples from sector III are all taken in the high strain belt.

## COMPARISON OF THE MEAN DYKE COMPOSITIONS OF SECTOR I, II AND III

The mean dyke compositions in Table V are calculated on the basis of samples from the centres of aphyric or originally aphyric dykes with $1.5 < FeO^*/MgO < 3.5$. In sector III a distinction has been made between dykes > 2 m and <2 m, i.e. dykes with or without a central zone according to the Kattsund dyke investigations. Based on the contents of the immobile elements (a.o. Y and Nb, see p. 50), the mean dykes of the three sectors are comparable, because they represent rocks in the same stage of differentiation.

With respect to major elements the mean dyke compositions can not directly be compared because of the calculation in per cent of the major element oxides. If there, for example, is a loss of one oxide, then the deficiency has to be added to the rest of the oxides in proportion to their amounts.

The comparisons can however be managed, if one element has been immobile during the metasomatic event, because then any oxide-X/oxide-immobile ratio will be constant if not oxide-X has been mobile (Pearce 1968, Zeck & Kalsbeek 1981). From many studies $Al_2O_3$ is suggested to be immobile (a.o. Beach 1973, 1976, Jamieson & Strong 1981, Kerrich *et al.* 1977, Morthorst *et al.* 1983, Zeck & Kalsbeek 1981). As this also appears to be the case in the present dykes, $Al_2O_3$ has been used as an immobile element.

The oxide-X/$Al_2O_3$ ratios and the trace element concentrations of the mean dykes have been exposed to statistical (t) testing. From this it is seen that the mean sector II dyke, the mean sector III dyke >2 m and the sector III dyke <2 m is highly significantly (the 1% level) enriched in FeO and highly significantly enriched in $Fe_2O_3$/FeO. Except for $H_2O$ there are no significant differences between the mean sector I dyke and the sector III dyke >2 m. The thin sector III dyke is highly significantly enriched in Rb and less significantly depleted in Sr and $FeO^*$.

## COMPARING THE INDIVIDUAL SECTOR II AND III SAMPLES TO THE MAGMATIC TRENDS OF THE SECTOR I DYKES

For direct comparison between the sector II and III samples and trends of the sector I samples oxide-X/$Al_2O_3$ and trace elements have been plotted

versus $TiO_2/Al_2O_3$ in variation diagrams. The $TiO_2/Al_2O_3$ ratio has been chosen as a substitute of the FeO*/MgO ratio because FeO* possibly in some cases has been mobile.

From the plots (Fig. 17) it is seen that there is a remarkable fit to the sector I variation of FeO*, $P_2O_5$, Y, Zr, Nb. In the rest of the diagrams some variation around the sector I trends is seen, but the plots of $Na_2O$, $K_2O$, Rb and Sr for the thin sector III dykes show deviations. $Na_2O$ is depleted in 4 of the thin dykes, and $K_2O$ and Rb are enriched in 6 of the samples (including the 4 $Na_2O$ depleted), but 4 others are within the igneous trend. Three of the thin dykes have lost part of their Sr.

The relations between K and Rb in the different groups of samples are shown in Fig. 18. The sector I and II samples define a narrow elliptic field trending slightly oblique to the mean igneous trend of Shaw (1968). In this group the K/Rb ratio varies from 189 to 366 with a mean K/Rb ratio of 259. The K/Rb ratio decreases with increasing K content. As seen from Fig. 18 B also the plot of the Kattsund dykes, the sector III >2 m dykes and the sector III <2 m dykes plot within narrow elliptical fields largely overlapping the field of the sector II and III dykes. Four of the K and Rb enriched thin sector III dykes extend the distribution to higher K and Rb values, but it is remarkable that these dykes plot on the extension of the trend of the sector I and II dykes.

### CONCLUSION

The alterations within the metamorphosed Koster dykes is restricted. The sector II and III dykes are enriched in $H_2O$, but besides this and a general enrichment in the $Fe_2O_3/FeO$ ratio of the sector II dykes, there can not be shown any general tendency of element mobility in the case of the sector II and sector III dykes >2 m. These dykes have compositions very close to their primary chemical composition. The thin dykes of the high strain zone have been changed to a certain extent. More than half of the dykes have been enriched in $K_2O$ and Rb. A little less than half of the dykes have been depleted in $Na_2O$, while about one third have been depleted in Sr.

## CHEMICAL ALTERATION IN THE MARGINAL ZONE OF THE KATTSUND DYKES

### PROFILES ACROSS KATTSUND DYKES

Three profiles have been investigated and in all three sections there are interior contact(s) to a slightly younger dyke. The profiles thus contain contacts

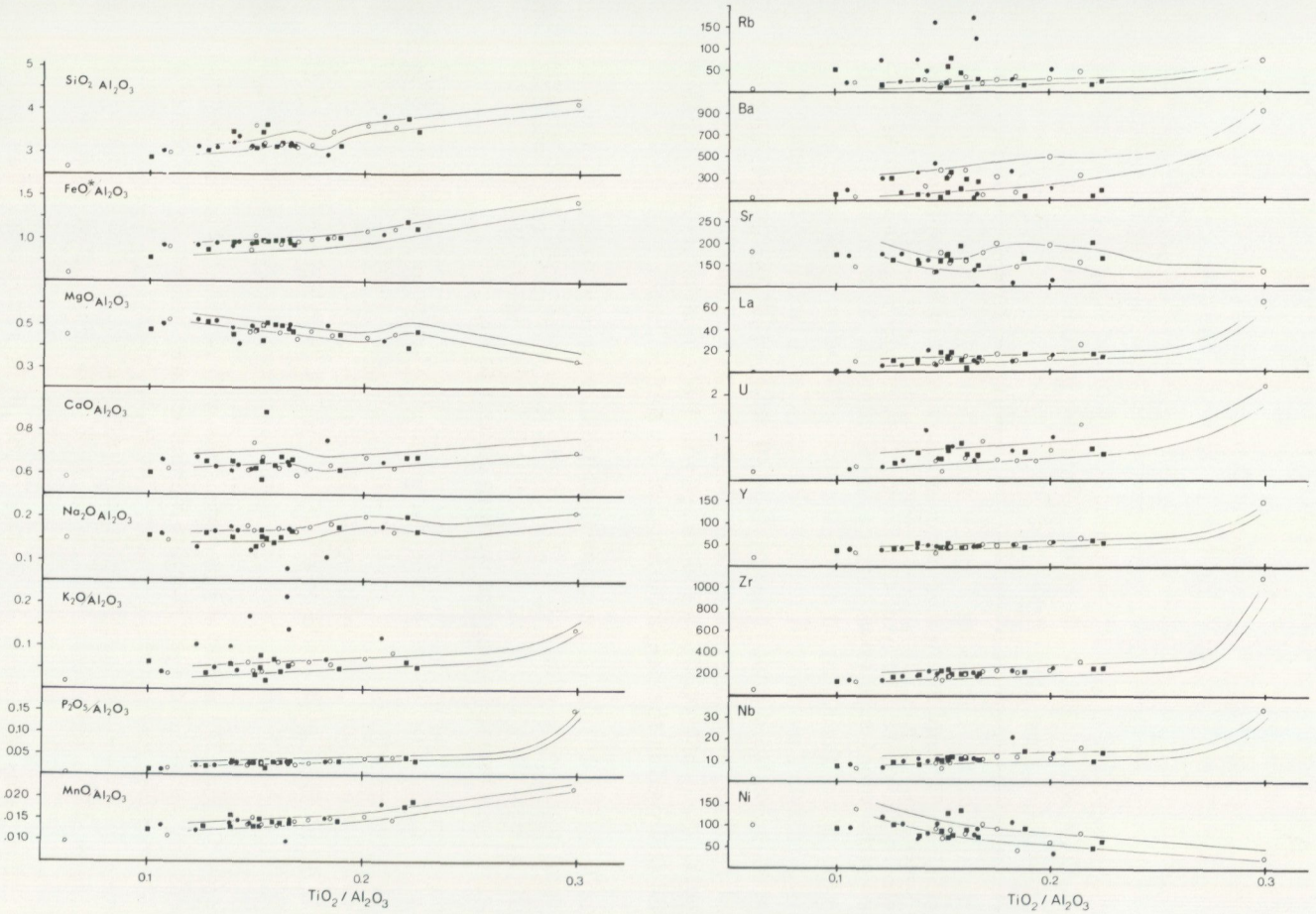


Fig. 17. Variation diagrams in which the samples of sector III dykes >2 m (squares), sector III dykes <2 m (filled circles) and sector II dykes (circles) are compared to the distribution of the sector I dykes delimited by the two trend lines of the diagrams.

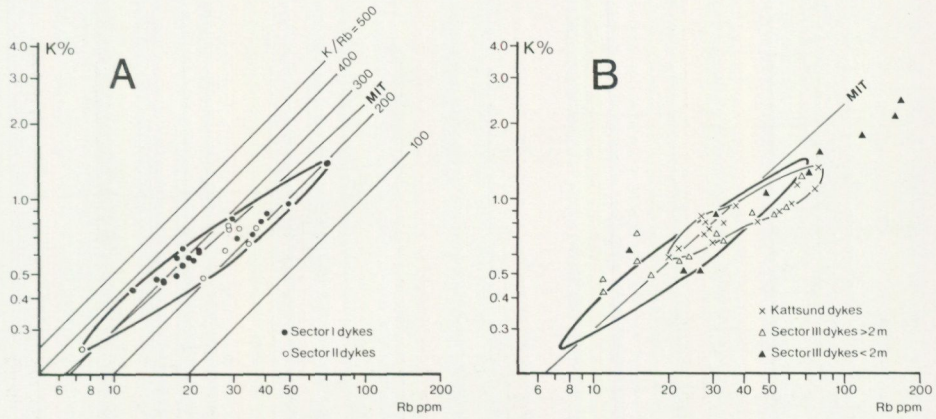


Fig. 18. Plot of K versus Rb. A) shows the distribution of the samples from sector I and II of the Koster area. The main igneous trend of Shaw (1968) is indicated as MIT. In B) the sector III dykes >2 m, the sector III dykes <2 m and the Kattsund dykes are compared to the distribution of the sector I and II dykes.

with high (the gneiss/dyke contact) as well as very low (the dyke/dyke contact) chemical gradients across. The textural considerations suggest that the rocks in the profiles originally were aphyric. No xenoliths in the dykes have been observed in the neighbourhood of the profile lines.

*Profile A* (Fig. 19) shows a multiple dyke with an exposed width of 5.5 m, but in total it may be as wide as 8 m. The central 2.5 m wide dyke shows mimetic chills against the older dyke, which itself is chilled against the host gneiss. Shearing is observed along the western contact to the gneiss.

*Profile B* (Fig. 20). In the profile two parallel dykes occur. The older dyke in the west is cut by a 5 m wide younger dyke with mimetic chills against both the gneiss and the older dyke. The eastern dyke contact is sheared, with an exceptionally strong degree of alteration associated with pyrite formation.

*Profile C* (Fig. 21) shows a 2 m wide dyke with decreasing grains size towards the gneiss. The dyke margins themselves are sheared. In the center a c. 10 cm wide younger dyke occurs. The main dyke of the profile is much thinner than the dyke complexes in profiles A and B. The thin younger dyke in the profile is represented by one analysis embracing the whole dyke.

The patterns of element distribution in the profiles show similarities, and it is obvious that the multiple dykes of profiles A and B have a *central zone* and

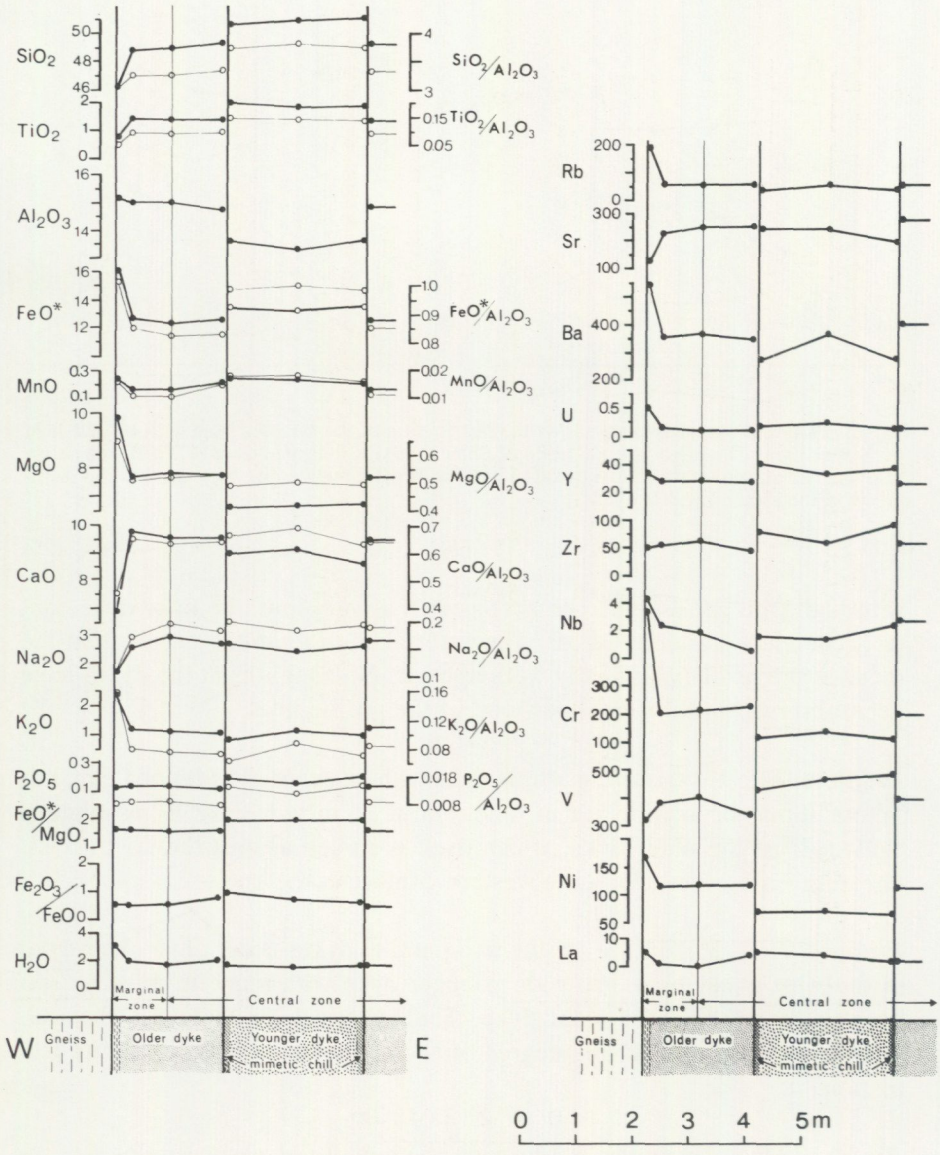


Fig. 19. Profile A, a profile across a multiple Kattsund dyke (see text).

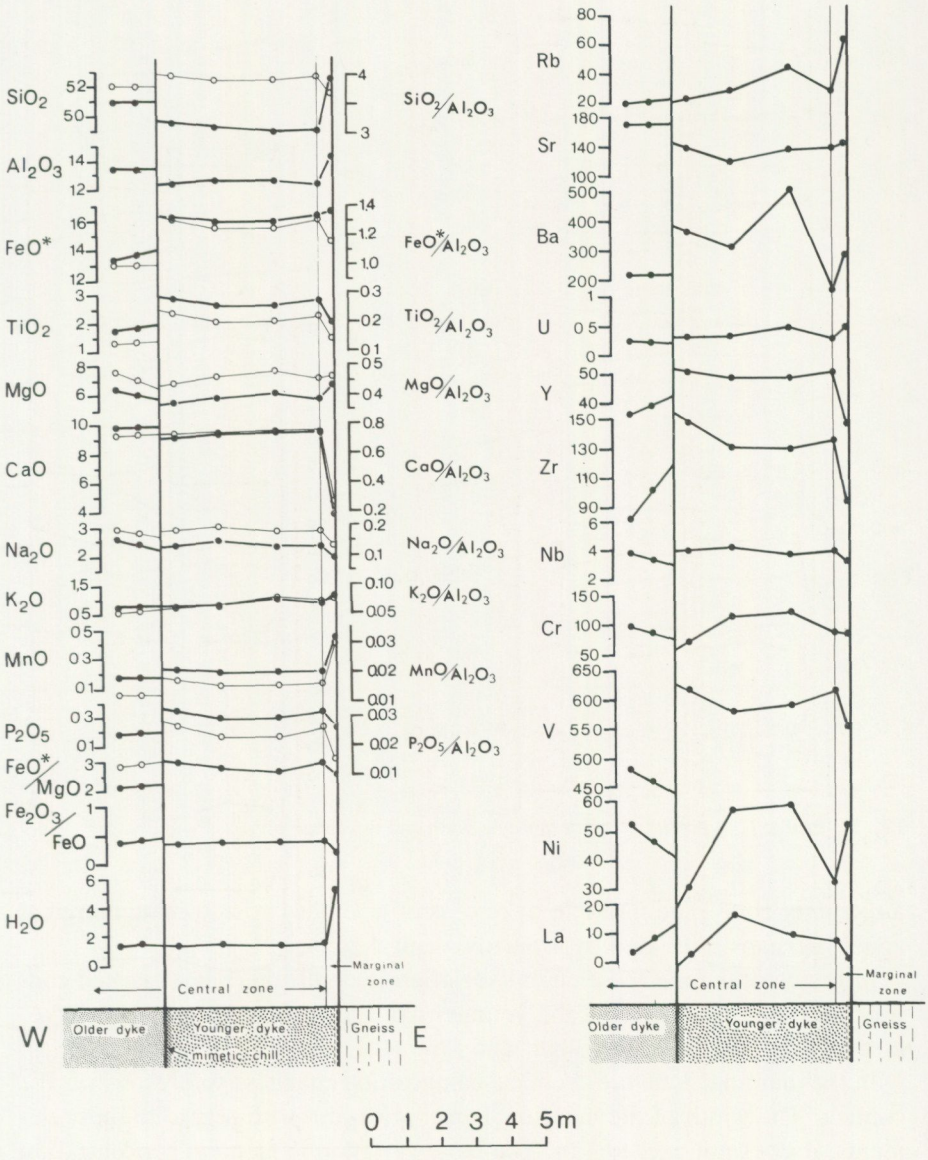


Fig. 20. Profile B, a profile across a multiple Kattsund dyke (see text).

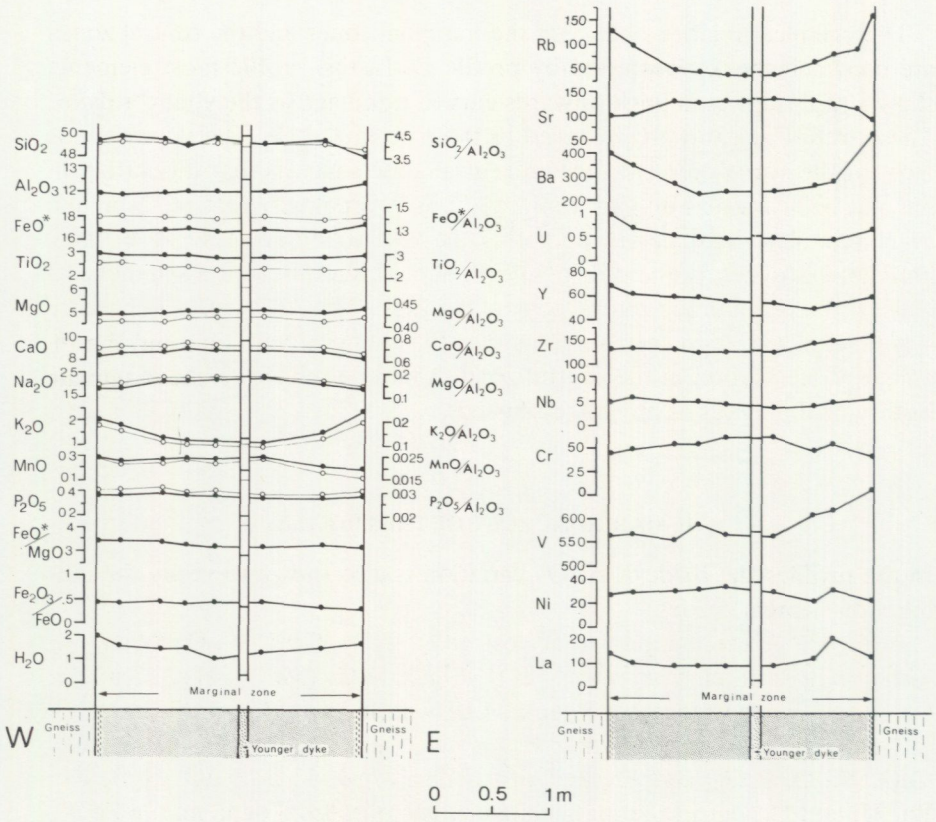


Fig. 21. Profile C, a profile across a multiple Kattsund dyke (see text).

a *marginal zone*. The multiple dyke of profile C has two adjoining marginal zones, perhaps separated by a narrow central zone.

In the central zone the element variation is small, there is a marked contrast between the older and the younger dyke rocks, and the younger dykes of profile A and B show a slight and symmetric element variation.

In the marginal zone the chemical composition changes rapidly towards the contact. The width of the marginal zone varies, but with regard to most elements, it does not exceed 1 m. The large variation in element concentration and the disagreement with magmatic trends shown by some elements indicate metasomatic changes which perhaps overshadow or include an effect from selective contamination of dyke margins. The non-magmatic element relations are for example seen in the marginal zone of profile A where FeO*, MgO, $K_2O$, MnO, Rb, Ba, U, La, Y, Nb, Cr and Ni increase, while $SiO_2$, $TiO_2$, CaO, $Na_2O$, Sr and V decrease and $Al_2O_3$, $P_2O_5$ are kept almost constant.

The chemical relations between the marginal zones and the central zones are convincingly demonstrated by profile B. In this profile most elements show a slight upwards or downwards curved trend across the younger dyke. These trends are abruptly changed in the marginal zone. The symmetry of most of the variation trends in the central zone suggests that this variation has not been formed by in/out migration as it is unlikely that metasomatic or contamination processes operating across two different types of rock boundaries (dyke/dyke and dyke/gneiss) should have created a symmetrical element variation in the central zone of the dyke. Thus the small and broadly symmetrical variation seen suggests that the chemical variation and the element concentration in the central zone should be related to the magmatic history of the dykes as already discussed.

## THE MARGINAL ZONE OF THE PROFILES

In the profiles the oxide-X/$Al_2O_3$ variation is also shown to verify the mobility of element oxides.

In profile A the marginal zone lost $SiO_2$, $TiO_2$, CaO, $Na_2O$, Sr and V, while there is an enrichment in FeO*, MgO, $K_2O$, (MnO), $H_2O$, Rb, Ba, Cr, and Ni. Furthermore the marginal zone is enriched in Cl (se Table IX).

The marginal zone in Profile B has also been depleted in $SiO_2$, $TiO_2$, CaO, $Na_2O$, $P_2O_5$, and Zr, and enriched in MgO, $K_2O$, MnO, $H_2O$, Rb, Ba, U, and Ni, but in the marginal zone, there is also a depletion in FeO*, $Fe_2O_3$, Y, Nb, Cl and a very strong enrichment in S (see Table X).

The two adjoining (?) marginal zones of profile C are less altered than the marginal zones of profile A and B. In the marginal zones of profile C, there is as in profile A and B seen a depletion in CaO, $Na_2O$ and an enrichment in $K_2O$, $H_2O$, Rb and Ba, but as in profile A Sr has been depleted and FeO* enriched. Cl has been enriched in both marginal zones of profile C and S has been depleted (for Cl & S see table XI).

The alteration seen in four marginal zones are of different degree and character. However CaO, $Na_2O$ have been lost and $K_2O$, $H_2O$, Rb, Ba have been enriched in all four margins. To get a better understanding of the kind of the metasomatic alterations in the margins of the Kattsund dykes, paired centre/margin samples have been studied.

## THE PAIRED SAMPLES

The concentrations of the trace elements and the oxide-X/$Al_2O_3$ ratios of the M, I and G type of paired samples (see p. 11–12 and Table XII) have been

plotted in (C, C-M) diagrams (Fig. 22). In this diagram the concentration (or oxide-X/$Al_2O_3$ ratio) of a given element in the samples from the centre of a dyke or a gneiss layer is shown by the abscissa (C-values). Along the ordinate is plotted the difference in the content (or oxide-X/$Al_2O_3$ ratio) between the corresponding samples from layer centre (C) and layer margin (M). If there is no difference between the centre and the margin, the paired samples will plot on the abscissa. C-M values >0 indicate depletion in the margin, while C-M values <0 indicate enrichment. In the (C, C-M) diagram a fan of lines is drawn. These lines show C-M values of 5, 10, 20 ... 200% of the C values.

Because the chilled dyke rock originally was slightly more evolved than the rock in the dyke centre, the plot of the M-pairs can not be expected initially to be located on the C-line. Judged from the variation diagrams (Fig. 6) and the I-pairs, the initial position of the various elements in the case of the Kattsund dyke M-pairs should be: 1) on the C-line ($SiO_2$, CaO, $Na_2O$, MnO), 2) above or possibly on the C-line (MgO, $K_2O$, Rb, Sr, Cr, Ni) and 3) below or eventually on the C-line (FeO*, $P_2O_5$, U, La, Y, Nb, Zr, V). The element migration across the boundary between the Kattsund dykes and the Sandbukta gneiss can be seen in the diagrams.

Based on the plot of the Kattsund dyke M-pairs the elements are divided into three groups. *Group I* includes highly mobile elements, while *Group II* includes elements, which have been mobile in some margins. *Group III* includes less mobile elements.

*Group I* includes $K_2O$, $Na_2O$, Rb, Ba, Sr, $H_2O$, Cl, and S. Most members of this group demonstrate nicely migration across the dyke/gneiss boundaries. Thus $K_2O$, Rb, Ba and $H_2O$ have moved from the margins of the gneiss layers and into the marginal zones of the Kattsund dykes. The opposite situation is seen in the case of $Na_2O$ and Sr. With respect to $H_2O$ the Kattsund dykes have been enriched throughout, but as seen the marginal zones are enriched relative to the central zones. Two of the Koster dyke pairs have the same content of alkalies in the dyke margins as in the dyke centres, while the two other pairs follow the Kattsund dyke pairs. Three of the Koster dyke pairs have in contrast to the Kattsund dykes lost an amount of Ba in the margins. Cl has been added to most of the Kattsund dyke margins, but it has also been depleted in a few. Thus the marginal zones of $M_5$ and $M_8$ have been strongly enriched and strongly depleted, respectively. Both $M_5$ and $M_8$ have been enriched in S in the dyke margins. Otherwise S has been depleted or enriched in the margins.

Fig. 22. C, (C—M) plot of M-pairs, G-pairs and I-pairs (see text). In most cases the value plotted is a multiplum of the real values and a factor, which is given in Appendix, p. 43. Filled circles = M-pairs, Kattsund; Circles = G-pairs, Kattsund; Squares = I-pairs, Kattsund; Triangles = M-pairs, Koster.

# GROUP I

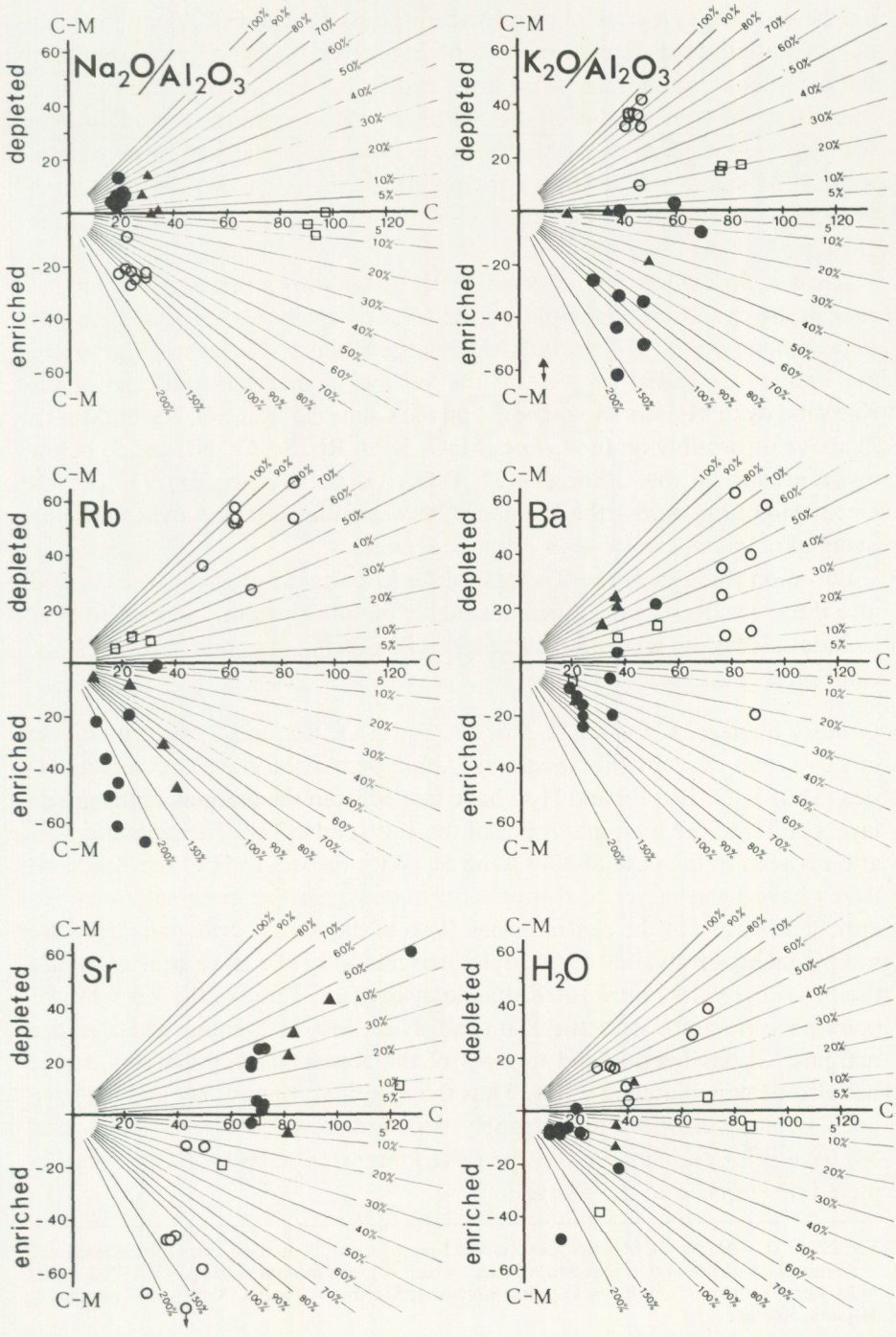
C-M
depleted
enriched
C-M
C
$Na_2O/Al_2O_3$
$K_2O/Al_2O_3$
Rb
Ba
Sr
$H_2O$
60
40
20
-20
-40
-60
5
10%
20%
30%
40%
50%
60%
70%
80%
90%
100%
150%
200%

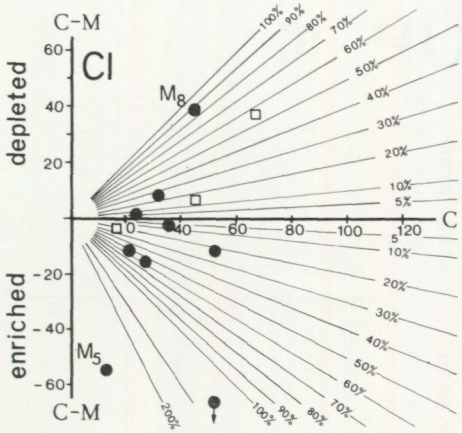
C-M
Cl
depleted
enriched
M8
M5
C
C-M

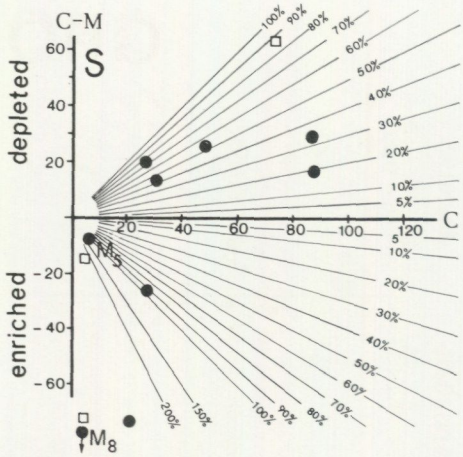
C-M
S
depleted
enriched
M5
M8
C
C-M

# GROUP II

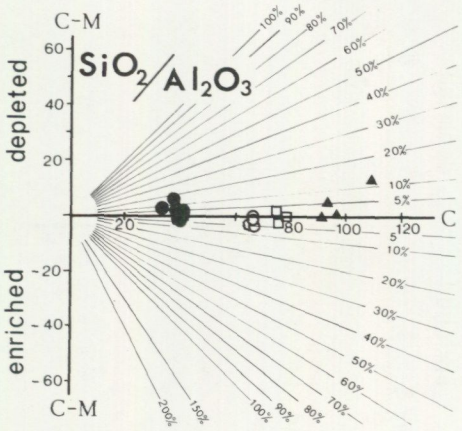
C-M
SiO2/Al2O3
depleted
enriched
C
C-M

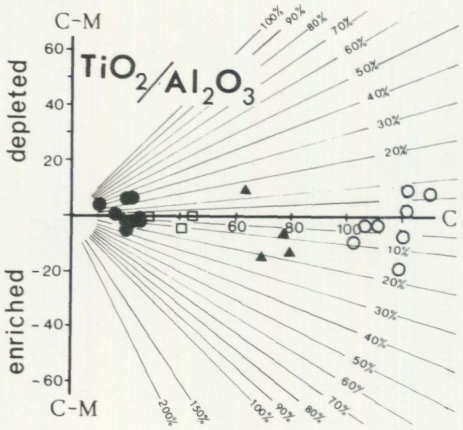
C-M
TiO2/Al2O3
depleted
enriched
C
C-M

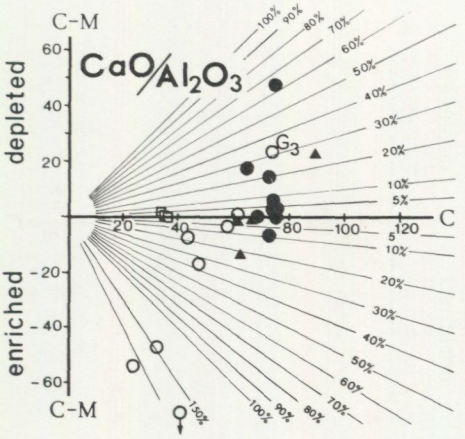
C-M
CaO/Al2O3
depleted
enriched
G3
C
C-M

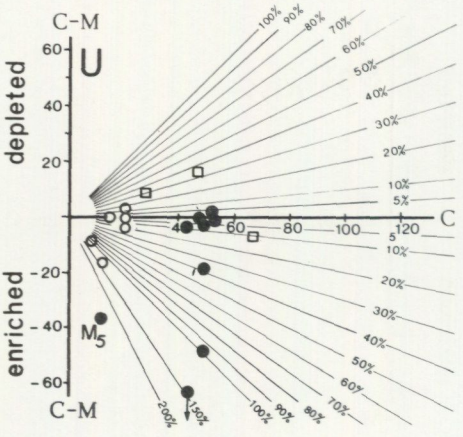
C-M
U
depleted
enriched
M5
C
C-M

# GROUP III

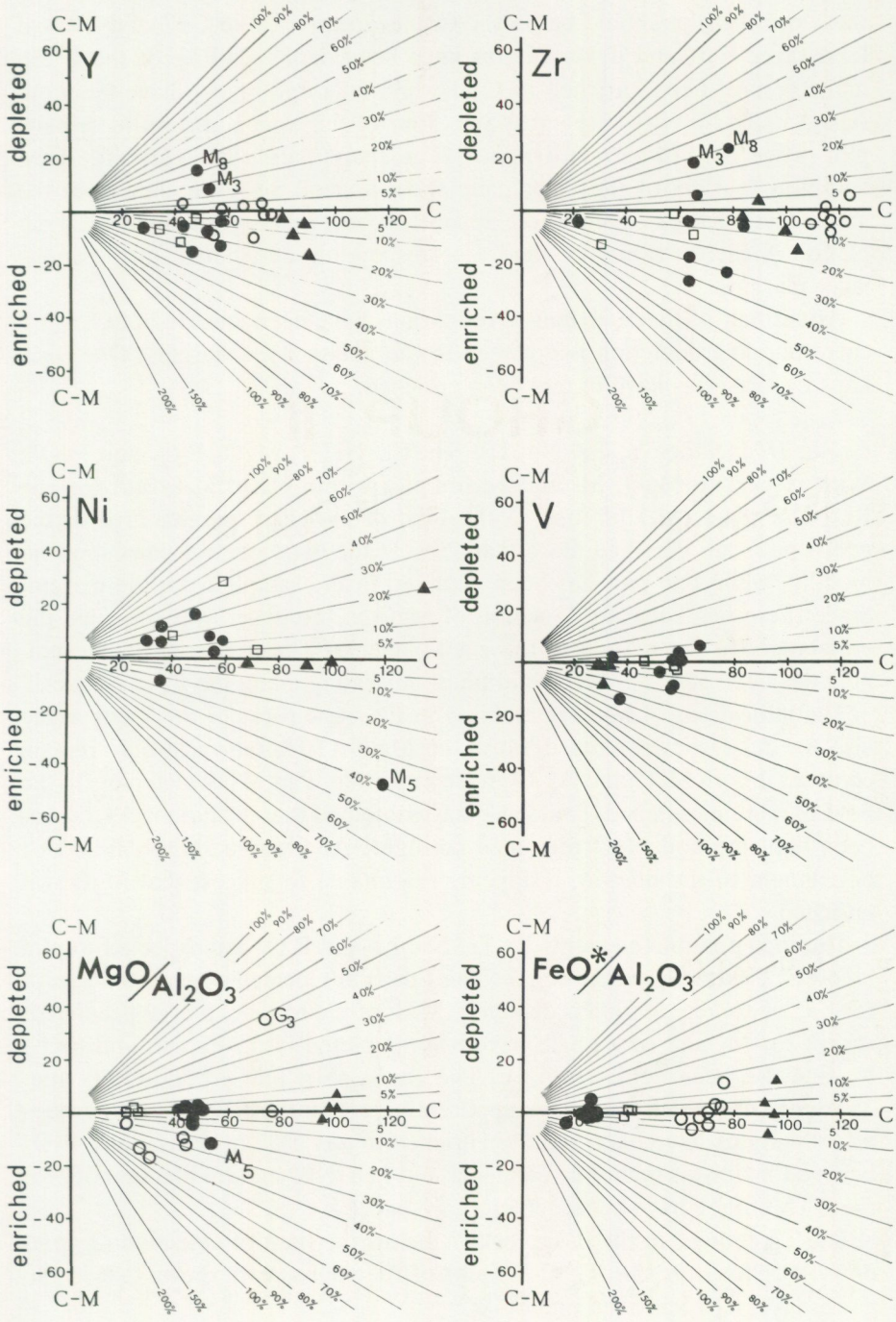
C-M
depleted
enriched
C-M
Y
Zr
Ni
V
MgO/Al2O3
FeO*/Al2O3
M8
M3
M5
G3
C
20
40
60
80
100
120
5
10%
20%
30%
40%
50%
60%
70%
80%
90%
100%
150%
200%
60
40
20
-20
-40
-60

*Group II* covers $SiO_2$, CaO, $TiO_2$ and U. $SiO_2$ and CaO are expected to have had the same content in the dyke margins as in the dyke centre and therefore the plot should be on the C line. In the case of CaO and $TiO_2$ at least three Kattsund dyke margins have been depleted. Five of the gneiss margins have been enriched in CaO while only one or two have been enriched in $TiO_2$. With respect to $SiO_2$ four of the nine Kattsund dyke pairs plot in the field of margin depleted. The gneiss pairs show very little C-M variation, but six of the eight pairs show a small $SiO_2$ enrichment in the gneiss layer margins. Thus there appears to be a weak tendency of $SiO_2$ depletion in the dyke margins and a corresponding enrichment in the gneiss layer margins.

About half of the Kattsund dyke margins have been enriched in U, but a corresponding depletion is not seen in the gneiss layer margins. One, perhaps two margins have in fact been enriched.

*Group III* includes Y, Zr, Nb, La, Th, Cr, Ni, V, MgO, $P_2O_5$ and FeO*. With respect to MgO, M- and I-pairs plot within C±10%, except for one Kattsund dyke ($M_5$) plotting in the field of enriched margin. Five of the gneiss pairs are enriched more than 20% in the margins, two pairs show no mobility while one pair has been depleted in the sample from the margin. Since there has been no depletion of MgO in the dyke layer margins, the enrichment in the margin of the gneiss layers indicates that MgO presumably has been added from a fluid phase migrating along the dyke contacts.

The indications of MgO immobility in the basic rocks of this study argue also for $Al_2O_3$ immobility because the MgO/$Al_2O_3$ ratio can only remain constant if both MgO and $Al_2O_3$ were immobile. Pair $M_5$, which plots in the field of margin enriched, could also have obtained that position if $Al_2O_3$ has been depleted and MgO remained constant. As $M_5$ also shows Ni and Cr enrichment in the margin, it appears reasonable to suggest that MgO was enriched.

The incompatible elements Y, Zr, Nb, La and $P_2O_5$ are expected to plot below or eventually on the C line. The I pairs are located as expected except for La, where one margin is depleted. Most of the M-pairs plot as predicted, except for $M_5$ and $M_8$, which have been depleted in Y, Zr, Nb and $P_2O_5$. $M_8$ has also been depleted in La. The gneiss pairs plot around the C line. Two gneiss layer margins have apparently been enriched in Y and perhaps a few margins have been slightly enriched in Zr. Y, Zr, Nb, La and $P_2O_5$ behaved mainly as immobile elements, but in a dyke margin like that of profile B ($M_8$) they have been depleted.

The Th content in the basic rocks is below the limit of detection (2 ppm) on XRF. However the (C, C-M) plot of the gneiss pairs shows that in the gneiss layers Th has been immobile.

The compatible elements Cr and Ni are originally expected to have been depleted in the margins, as indicated by the I pairs. Except for $M_5$ (the profile A), which is strongly enriched in the margin, Cr and Ni have been immobile. The content of Cr and Ni in the gneiss layers is below the limit of detection (2 ppm). The original position of the M pairs is in the case of FeO* and V expected to be on or below the C line as indicated by the I pairs. FeO* may have been slightly enriched or depleted in a few of the Kattsund dyke margins, but generally it has been immobile. V has been immobile, perhaps slightly depleted in one or two of the Kattsund dyke margins. The vanadium content in the gneiss layers is below the limit of detection (2 ppm).

## CONCLUSIONS ON THE STUDY OF THE ALTERATIONS IN THE KATTSUND DYKES

The metasomatic alterations of the Kattsund dykes are essentially restricted to the marginal zones of the dykes. The study demonstrates that the metasomatism has a fundamental component of element migration across the dyke-gneiss boundary, as the marginal zones of the gneiss and dyke layers are depleted/enriched or enriched/depleted, respectively, with respect to a certain element.

The central zones have been enriched in $H_2O$ by inwards migrating $H_2O$. As this $H_2O$ enrichment has happened without important influence on the igneous element composition of the central zones, it can be concluded *that the marginal zones acted as filters absorbing inwards migrating elements of the fluid phase.*

The metasomatic alterations in the marginal zones themselves are complex and almost all elements have been involved in migration. The samples from the marginal zones in pairs $M_2$, $M_3$, $M_5$ and $M_8$ have undergone the strongest metasomatic alteration and commonly they show the highest mobility of the elements. The marginal zone of $M_8$ (profile B) shows generally deviating direction of element mobility. $M_3$ follows partly $M_8$.

Besides the common tendencies of element movements the investigations of both the profiles and the paired samples demonstrate, that at least three types of alteration of the dyke margins are seen. In the common type of alteration $SiO_2$, $TiO_2$, CaO, $Na_2O$, $Fe_2O_3$/FeO and Sr have been reduced in the marginal zone, while $K_2O$, $H_2O$, Rb, Ba, U, (La), Cl have been enriched. This type of alteration is seen in the dyke of profile C.

The second type of alteration can be seen in the marginal zones of profile A ($M_5$) and this type deviates from the common type by also being depleted in V and Zr and enriched in FeO*, MgO, Cr and Ni. In that margin $Fe_2O_3$/FeO is unchanged and there is an S enrichment.

The third type of alteration seen in the marginal zone of profile B ($M_8$) deviates strongly from the common type by also being depleted in FeO*, $P_2O_5$, Y, Zr, Nb, V and Cl and enriched in MgO, MnO, Sr, Cr (?) and Ni. It is the only marginal zone which has been enriched in MnO and Sr and one of the few depleted in $P_2O_5$, FeO*, Y, Zr, Nb (?). Furthermore it shows only a little enirchment in $K_2O$, while it shows the strongest depletion in CaO and Cl and the strongest enrichment in $H_2O$ and S.

The existence of these types suggests that more than one metasomatic event has existed, and these events may have been separated in time. Even in one and the same margin, one can not be sure, that the chemical variation seen is only due to one event. The well developed planar fabric in the dyke margins makes the dyke margins to mechanically weak zones in the rock mass. Any stress situation to be relaxed could be relaxed by movements in one or several or the dyke margins and then guide the penetration of a fluid phase. The two generations of biotite followed by a chlorite replacement which can be seen close to the contacts of the Kattsund dykes support the complexity of the processes in the dyke margin.

## COMPARISON OF THE METASOMATIC CHANGES OF THE KATTSUND AND THE KOSTER DYKES WITH OTHER METASOMATICALLY ALTERED BASIC DYKE ROCKS

Chemical alterations of doleritic/gabbroic rocks exposed to amphibolite facies metamorphism have been studied by Elliott (1973), Field and Elliott (1974), Zeck and Kalsbeek (1981) and Morthorst *et al.* (1984). The result of these investigations is together with the result of the present investigation summarized in Fig. 23.

The rocks studied by Elliott (1973), Field and Elliott (1974) and by Morthorst *et al.* (1983) are like the rocks of this study situated within the Sveconorwegian province. Elliott (1973) and Field and Elliott (1974) studied the chemical alterations within the classical 'hyperites' of S Norway, while Morthorst *et al.* (1983) studied the "hyperites" of Värmland, W Sweden. Both groups of hyperites were injected into quartzo-feldspathic gneisses belonging to the amphibolite facies and they were both exposed to Sveconorwegian amphibolite facies metamorphism (Starmer 1972, Morthorst *et al.* 1983). The Kangamiut dykes, W Greenland, studied by Zeck and Kalsbeek (1981), intruded into a thick granulite facies sialic crust about 1950 Ma ago (Kalsbeek *et al.* 1978) and became deformed and amphibolitised during the Nagssugtoquidian orogeny (c. 1800 Ma).

When the results of the different investigations are compared it is impor-

| | 1 | 2 | 3 | 4 | 5 | 6 | 7 |
|---|---|---|---|---|---|---|---|
| $SiO_2$ | i | i | i | – | (–) | – | i |
| $TiO_2$ | i | i | | – | i | i | i |
| $Al_2O_3$ | i | i | | i | i | i | i |
| MnO | i | i | i | (±) | i | (+) | (+) |
| MgO | i | i | i | i | i | i | i |
| CaO | i | i | (–) | – | – | + | i |
| $Na_2O$ | i | i | – | – | i | – | + |
| $K_2O$ | i | (+) | + | + | + | (+) | + |
| $P_2O_5$ | i | i | i | – | + | i | i |
| FeO* | i | – | i | (±) | i | + | i |
| $Fe_2O_3/FeO$ | i | i | i | – | + | – | + |
| $H_2O$ | + | + | + | + | + | + | + |
| Rb | i | + | + | + | + | – | + |
| Ba | i | i | (–) | + | ± | – | (+) |
| Sr | i | – | – | – | ± | – | i |
| La | i | i | i | + | (i) | | |
| Y | i | i | i | (–) | i | i | i |
| U | i | i | i | + | i | – | |
| Th | | | | | i | – | + |
| Zr | i | i | i | (–) | + | – | i |
| Nb | i | i | i | (–) | i | – | |
| Ni | i | i | i | i | i | i | i |
| V | i | i | i | i | + | | |
| Cr | i | i | i | i | (i) | | |
| Cl | | | | ± | + | | + |
| S | | | | ± | – | | – |

Fig. 23. Observed element mobility connected to the metasomatic alterations of the Kattsund dykes, the Koster dykes, and other basaltic rocks exposed to amphibolite facies metasomatism. i = immobile, + = enriched, – = depleted.

1) Koster amphibolites >2 m of sector III
2) Koster amphibolites <2 m of sector III
3) Element mobility in the Koster amphibolites found by comparing individual samples to the variation trends of the sector I dykes.
4) Marginal zones of the Kattsund dykes
5) S Norwegian hyperites (Elliott 1973, Field and Elliott 1974).
6) Kangamiut dyke swarm (Zeck & Kalsbeek 1981)
7) Värmland hyperites (Morthorst *et al.* 1983).

tant to have in mind that several factors could have caused differences in the nature of the metasomatism. Such factors are a.o.: differences in the composition of the fluid phase involved, the amounts of fluid phase penetrating the dyke rock, differences in PT conditions, the chemical composition of the host rock (see Fratta & Shaw 1974, Morthorst *et al.* 1983, Rock *et al.* 1985).

The methods used in the evaluation of the metasomatic changes are: 1) paired samples (Elliott 1973, Field & Elliott 1974, Morthorst *et al.* 1984, this paper), 2) comparing the mean composition of altered rocks to the mean composition of equivalent fresh rocks (Zeck & Kalsbeek 1981, this paper), 3) comparing individual samples to magmatic variation trends established from the fresh samples (Zeck & Kalsbeek 1981, Morthorst *et al.* 1983, this paper). In the studies of the major elements Zeck and Kalsbeek (1981) and Morthorst *et al.* use MgO as an immobile element oxide in their study while Elliott (1973) does not concider the problem with the constant sum effect of the oxides.

The methods of paired samples in the investigations of Elliott (1973), Field & Elliott (1974), and Morthorst *et al.* (1983) are based on the assumption of no primary chemical differences between the fresh rock and the altered rock. In the present investigation it has been attempted to eliminate this source of error.

Comparing the four different investigations of Fig. 23, it is seen that elements as $SiO_2$, CaO, $Na_2O$, Sr, Ba, and S may be expected to migrate out of the basic rock under amphibolite facies metasomatism, while (MnO), $K_2O$, $H_2O$, Rb, Ba, and Cl may enter the basic rock. $A1_2O_3$, MgO, $TiO_2$, $P_2O_5$, Y, Zr, Nb, Zr, Ni will in general be immobile, but if a little mobility is shown by $TiO_2$, $P_2O_5$, Y, Zr, and Nb, it will presumably be directed out of basic rock.

ACKNOWLEDGEMENTS

The author wants to thank F. Kalsbeek, P.M. Holm and S. Pedersen for stimulating discussions and critical reading of the manuscript. Furthermore thanks are given to Aa. Jensen who studied the Fe-Ti-oxides and to the Laboratories at GGU (I. Sørensen and J. Kystol), at Institute of Petrology (J. Bailey) and to the Risø National Laboratory. Thanks is also given to L. Samuelsson for his help collecting the LS samples and interest in the study. The study was financially supported by the Danish Natural Science Research Council.

## APPENDIX

### ANALYTICAL METHODS ETC.

The major and minor elements have been analysed in the chemical laboratories of the Geological Survey of Greenland (GGU) using a Siemens SRS XRF-spectrometer. The methods used are outlined by Sørensen (1975, 1976). The $Fe_2O_3/FeO$ ratio was determined by wet chemistry while the $Na_2O$ and MgO were determined by atomic absorbtion spectrometry. $H_2O$ contents were determined by the Penfield method.

The trace elements were analysed at the Institute of Petrology, Copenhagen University, by the XRF methodes outlined by Norrish & Chappell (1967) using a Phillips PW 14/10 semi-automatic XRF spectrometer and a Phillips automatic PX 1410 spectrometer. U has been determined at Risø National Laboratory by delayed neutron counting.

The precision of the determinations of trace element contents given by the laboratories are: U (±3—5%), Rb (±0.5—3 ppm), Sr (0.5—3 ppm), La (2—3 ppm), Y (1—3 ppm), Th (1—2 ppm), Zr (1—3 ppm), Nb (0.5—2 ppm), Ni (3—6 ppm), V (3—6 ppm), Cr (3—6 ppm), Cl (±10%) and S (±10 ppm).

In the table oxide analyses are recalculated free of L.O.I. and the CIPW norms are calculated using a fixed $Fe_2O_3/FeO = 0.15$ as proposed by Brooks (1976).

Factors used in connection with the (C, C-M) plot in Fig. 22.

| | M-pair Kattsund dyke | M-pair Koster dyke | I-pair | G-pair |
|---|---|---|---|---|
| $SiO_2$ | 10 | 30 | 20 | 10 |
| $TiO_2$ | 10 | $5 \cdot 10^2$ | $2 \cdot 10^2$ | $10^4$ |
| MgO | $10^2$ | $2 \cdot 10^2$ | 50 | $5 \cdot 10^3$ |
| CaO | $10^2$ | $10^2$ | 50 | $10^3$ |
| $Na_2O$ | $10^2$ | $2 \cdot 10^2$ | $5 \cdot 10^2$ | $10^2$ |
| $K_2O$ | $5 \cdot 10^2$ | $5 \cdot 10^2$ | $10^2$ | $10^2$ |
| FeO* | 20 | $10^2$ | 30 | $5 \cdot 10^2$ |
| $H_2O$ | 10 | 20 | 50 | $10^2$ |
| Rb | 0.5 | 0.5 | 0.5 | 0.33 |
| Ba | $10^{-1}$ | $10^{-1}$ | $10^{-1}$ | $10^{-1}$ |
| La | 2 | 2 | 2 | – |
| Y | – | 2 | – | – |
| U | $10^2$ | | $10^2$ | 4 |
| Zr | 0.5 | 0.5 | 0.5 | 0.5 |
| V | $10^{-1}$ | $10^{-1}$ | $10^{-1}$ | |

Table I. Mean composition of the Sandbukta gneiss. N=9. Oxides in weight%, elements in ppm.

| | $\bar{x}$ | s |
|---|---|---|
| $SiO_2$ | 76.70 | 0.89 |
| $TiO_2$ | 0.14 | 0.09 |
| $Al_2O_3$ | 11.61 | 0.13 |
| $Fe_2O_3$ | 0.46 | 0.13 |
| FeO | 1.23 | 0.14 |
| MnO | 0.03 | 0.01 |
| MgO | 0.16 | 0.14 |
| CaO | 0.55 | 0.18 |
| $Na_2O$ | 2.80 | 0.38 |
| $K_2O$ | 5.08 | 0.33 |
| $P_2O_5$ | 0.01 | 0.01 |
| FeO* | 1.64 | 0.09 |
| $H_2O$ | 0.24 | 0.50 |

| | $\bar{x}$ | s |
|---|---|---|
| Rb | 194 | 24 |
| Ba | 831 | 65 |
| Sr | 41 | 7 |
| La | 60 | 9 |
| Y | 70 | 5 |
| U | 4 | 1 |
| Th | 15 | 2 |
| Zr | 232 | 10 |
| Nb | 21 | 1 |
| Ni | 4 | 1 |
| V | <3 | |
| Cr | <3 | |
| | | |

Table II. Samples from the centres of Kattsund dykes ≥2.5 m wide. Oxides in weight %, elements in ppm.

| | 40801 | 40802 | 40803 | 40805 | 40806 | 40813 | 40846 | 40850 | 40853 |
|---|---|---|---|---|---|---|---|---|---|
| $SiO_2$ | 51.05 | 51.12 | 49.40 | 50.98 | 49.42 | 49.60 | 49.03 | 49.72 | 49.03 |
| $TiO_2$ | 1.77 | 1.84 | 2.57 | 1.90 | 1.46 | 2.84 | 1.44 | 1.08 | 2.58 |
| $Al_2O_3$ | 13.25 | 13.48 | 12.73 | 13.31 | 14.74 | 12.12 | 15.03 | 15.53 | 12.72 |
| $Fe_2O_3$ | 4.32 | 3.88 | 4.38 | 3.91 | 3.75 | 5.33 | 2.69 | 2.46 | 4.22 |
| FeO | 9.65 | 10.24 | 12.00 | 10.06 | 9.25 | 12.03 | 9.97 | 9.04 | 12.18 |
| MnO | 0.27 | 0.17 | 0.20 | 0.24 | 0.22 | 0.28 | 0.17 | 0.15 | 0.20 |
| MgO | 6.87 | 6.06 | 5.80 | 6.70 | 7.78 | 5.23 | 7.83 | 8.25 | 6.11 |
| CaO | 8.85 | 9.86 | 9.32 | 9.16 | 9.47 | 8.89 | 9.54 | 9.49 | 9.40 |
| $Na_2O$ | 2.20 | 2.39 | 2.52 | 2.47 | 2.72 | 2.20 | 3.01 | 2.84 | 2.29 |
| $K_2O$ | 1.60 | 0.76 | 0.79 | 1.13 | 1.07 | 1.13 | 1.14 | 1.33 | 0.98 |
| $P_2O_5$ | 0.18 | 0.19 | 0.30 | 0.16 | 0.12 | 0.37 | 0.14 | 0.10 | 0.29 |
| FeO* | 13.53 | 13.73 | 15.93 | 13.57 | 12.63 | 16.82 | 12.39 | 11.25 | 15.98 |
| FeO*/MgO | 1.97 | 2.27 | 2.75 | 2.03 | 1.62 | 3.22 | 1.58 | 1.36 | 2.62 |
| $Fe_2O_3$/FeO | 0.45 | 0.38 | 0.36 | 0.39 | 0.41 | 0.44 | 0.27 | 0.27 | 0.35 |
| $H_2O$ | 2.05 | 1.48 | 1.53 | 1.73 | 2.15 | 1.00 | 1.80 | 1.90 | 1.40 |
| | | | | | | | | | |
| Rb | 79 | 22 | 30 | 60 | 57 | 37 | 62 | 77 | 45 |
| Ba | 422 | 235 | 319 | 372 | 351 | 242 | 369 | 227 | 575 |
| Sr | 188 | 170 | 123 | 246 | 256 | 136 | 253 | 357 | 137 |
| La | 5 | 8 | 16 | 4 | 4 | 9 | 1 | 1 | 9 |
| Y | 35 | 38 | 48 | 34 | 28 | 57 | 29 | 21 | 48 |
| U | 0.360 | 0.270 | 0.318 | 0.240 | 0.120 | 0.488 | 0.118 | 0.090 | 0.474 |
| Th | <2 | <2 | <2 | <2 | <2 | <2 | <2 | <2 | <2 |
| Zr | 65 | 96 | 131 | 61 | 43 | 127 | 63 | 45 | 130 |
| Nb | 1.7 | 3.4 | 4.2 | 1.4 | 0.6 | 4.3 | 1.9 | 1.5 | 3.7 |
| Ni | 62 | 46 | 57 | 71 | 119 | 35 | 118 | 138 | 59 |
| V | 424 | 461 | 580 | 470 | 345 | 569 | 406 | 347 | 590 |
| Cr | 149 | 89 | 117 | 139 | 228 | 62 | 216 | 241 | 127 |
| | | | | | | | | | |
| CIPW NORM | | | | | | | | | |
| Q | 2.66 | 1.62 | | | | 1.75 | | | |
| Or | 9.45 | 4.52 | 4.65 | 6.66 | 6.34 | 6.69 | 6.72 | 7.88 | 5.81 |
| Ab | 18.65 | 20.30 | 21.37 | 20.91 | 23.03 | 18.64 | 25.31 | 24.05 | 19.40 |
| An | 21.55 | 23.82 | 21.15 | 21.97 | 24.92 | 19.94 | 24.17 | 25.72 | 21.58 |
| Nc | | | | | | | 0.10 | | |
| Di | 17.27 | 19.92 | 19.47 | 18.64 | 17.60 | 18.45 | 18.34 | 16.99 | 19.44 |
| Hy | 20.37 | 23.23 | 24.05 | 25.06 | 8.33 | 25.05 | | 2.33 | 23.25 |
| Ol | | | | 0.16 | 14.30 | | 19.91 | 18.57 | 1.88 |
| Mt | 6.26 | 2.64 | 3.06 | 2.61 | 2.42 | 3.23 | 2.38 | 2.16 | 3.07 |
| Il | 3.37 | 3.51 | 4.89 | 3.62 | 2.78 | 5.40 | 2.74 | 2.06 | 4.92 |
| Ap | 0.43 | 0.45 | 0.69 | 0.38 | 0.29 | 0.85 | 0.33 | 0.24 | 0.66 |

Continued table II.

| | 40866 | 40872 | 40874 | 7415 | 7425 | 10823 | 10827 |
|---|---|---|---|---|---|---|---|
| $SiO_2$ | 49.86 | 50.29 | 48.84 | 48.57 | 49.39 | 49.41 | 49.22 |
| $TiO_2$ | 2.57 | 2.02 | 2.82 | 2.87 | 2.85 | 2.32 | 2.77 |
| $Al_2O_3$ | 12.73 | 12.98 | 12.52 | 12.56 | 12.87 | 14.00 | 12.55 |
| $Fe_2O_3$ | 4.03 | 3.98 | 4.68 | 4.18 | 4.28 | 3.33 | 4.63 |
| FeO | 11.99 | 11.02 | 12.09 | 13.22 | 12.61 | 12.02 | 12.47 |
| MnO | 0.19 | 0.19 | 0.20 | 0.29 | 0.30 | 0.25 | 0.31 |
| MgO | 5.65 | 6.49 | 5.78 | 5.67 | 5.05 | 5.73 | 5.28 |
| CaO | 9.16 | 9.37 | 9.42 | 9.13 | 9.08 | 9.22 | 8.92 |
| $Na_2O$ | 2.55 | 2.07 | 2.63 | 2.13 | 2.22 | 2.67 | 2.43 |
| $K_2O$ | 0.97 | 1.39 | 0.70 | 1.03 | 0.92 | 0.87 | 0.96 |
| $P_2O_5$ | 0.30 | 0.19 | 0.30 | 0.36 | 0.44 | 0.18 | 0.45 |
| FeO* | 15.62 | 14.60 | 14.31 | 14.98 | 16.46 | 15.02 | 16.64 |
| FeO*/MgO | 2.76 | 2.25 | 2.82 | 2.99 | 3.26 | 2.62 | 3.15 |
| $Fe_2O_3$/FeO | 0.34 | 0.36 | 0.39 | 0.32 | 0.34 | 0.28 | 0.37 |
| $H_2O$ | 1.41 | 1.44 | 1.06 | 1.53 | 1.19 | 1.48 | 0.58 |
| | | | | | | | |
| Rb | 28 | 65 | 20 | 27 | 29 | 28 | 33 |
| Ba | 343 | 368 | 221 | 236 | 373 | 356 | 196 |
| Sr | 141 | 143 | 145 | 131 | 163 | 126 | 112 |
| La | 7 | 5 | 6 | 10 | 10 | 9 | |
| Y | 46 | 43 | 53 | 56 | 55 | 53 | 42 |
| U | 0.433 | 0.523 | 0.493 | 0.562 | 0.393 | | 0.674 |
| Th | <2 | <2 | <2 | <2 | <2 | <2 | <2 |
| Zr | 126 | 112 | 155 | 134 | 134 | 121 | 115 |
| Nb | 4.8 | 3.0 | 5.0 | 4.4 | 4.2 | 3.6 | 5.3 |
| Ni | 35 | 55 | 54 | 54 | 53 | 41 | 40 |
| V | 564 | 515 | 373 | 594 | 561 | 502 | 578 |
| Cr | 156 | 123 | 116 | 107 | 119 | 84 | 87 |
| CIPW NORM | | | | | | | |
| Q | 0.13 | 0.05 | | 0.07 | 2.06 | | 0.60 |
| Or | 5.74 | 8.22 | 4.15 | 6.08 | 5.45 | 5.08 | 5.68 |
| Ab | 21.62 | 17.57 | 22.31 | 18.09 | 18.83 | 22.34 | 20.59 |
| An | 20.47 | 22.05 | 20.34 | 21.70 | 22.49 | 23.40 | 20.58 |
| Di | 19.35 | 19.36 | 20.54 | 17.90 | 16.63 | 17.22 | 17.54 |
| Hy | 24.12 | 25.64 | 20.40 | 26.63 | 24.94 | 18.94 | 25.50 |
| Ol | | | 3.04 | | | 4.18 | |
| Mt | 3.00 | 2.80 | 3.13 | 3.26 | 3.16 | 2.85 | 3.20 |
| Il | 4.89 | 3.85 | 5.38 | 5.45 | 5.42 | 4.37 | 5.28 |
| Ap | 0.69 | 0.45 | 0.71 | 0.83 | 1.02 | 0.42 | 1.04 |
| Cc | | | | | | 0.02 | |

Table III. Samples of Koster dykes from sector I. Oxides in weight %, elements in ppm.

| | 41111 | 41112 | 41113 | 41114 | 41115 | 41123 | 41124 | 41125 | 41128 |
|---|---|---|---|---|---|---|---|---|---|
| $SiO_2$ | 49.97 | 48.39 | 47.60 | 48.64 | 48.52 | 47.95 | 47.68 | 48.66 | 48.46 |
| $TiO_2$ | 2.49 | 2.29 | 2.64 | 3.13 | 2.34 | 30.5 | 2.42 | 3.38 | 3.53 |
| $Al_2O_3$ | 14.74 | 14.49 | 14.84 | 12.92 | 14.69 | 13.39 | 14.84 | 12.35 | 11.86 |
| $Fe_2O_3$ | 2.40 | 3.18 | 2.67 | 3.11 | 2.32 | 2.95 | 2.33 | 3.18 | 2.73 |
| FeO | 12.15 | 11.03 | 12.22 | 12.94 | 11.78 | 12.84 | 11.99 | 13.65 | 14.53 |
| MnO | 0.21 | 0.20 | 0.21 | 0.23 | 0.20 | 0.22 | 0.20 | 0.24 | 0.25 |
| MgO | 6.83 | 7.01 | 7.10 | 5.72 | 6.86 | 6.15 | 7.25 | 5.30 | 4.40 |
| CaO | 9.77 | 10.05 | 9.56 | 9.53 | 9.63 | 9.79 | 9.83 | 9.29 | 8.71 |
| $Na_2O$ | 2.21 | 2.33 | 1.92 | 2.24 | 2.37 | 2.23 | 2.24 | 2.21 | 2.22 |
| $K_2O$ | 0.75 | 0.65 | 0.70 | 0.97 | 0.83 | 0.87 | 0.70 | 1.05 | 1.66 |
| $P_2O_5$ | 0.47 | 0.36 | 0.49 | 0.59 | 0.45 | 0.56 | 0.53 | 0.68 | 1.61 |
| FeO* | 14.31 | 13.89 | 14.62 | 15.74 | 13.87 | 15.50 | 14.09 | 16.51 | 16.99 |
| FeO*/MgO | 2.10 | 1.98 | 2.06 | 2.75 | 2.02 | 2.52 | 1.94 | 3.12 | 3.86 |
| $Fe_2O_3$/FeO | 0.20 | 0.29 | 0.22 | 0.24 | 0.20 | 0.23 | 0.19 | 0.23 | 0.19 |
| $H_2O$ | 0.58 | 0.57 | 1.36 | 0.37 | 0.87 | 1.15 | 0.57 | 0.73 | 0.56 |
| | | | | | | | | | |
| Rb | 22 | 19 | 18 | 39 | 31 | 36 | 20 | 41 | 71 |
| Ba | 291 | 236 | 237 | 514 | 260 | 484 | 272 | 586 | 818 |
| Sr | 175 | 151 | 170 | 140 | 164 | 131 | 170 | 133 | 131 |
| La | 13 | 8 | 12 | 17 | 15 | 22 | 15 | 25 | 59 |
| Y | 48 | 46 | 46 | 63 | 48 | 63 | 51 | 73 | 129 |
| U | 0.493 | 0.398 | 0.463 | 0.952 | 0.739 | 0.850 | 0.519 | 1.07 | 2.07 |
| Th | <2 | <2 | <2 | <2 | <2 | 3 | <2 | <2 | 3 |
| Zr | 223 | 189 | 223 | 274 | 230 | 267 | 240 | 326 | 850 |
| Nb | 13 | 8.7 | 12 | 14 | 11 | 13 | 13 | 16 | 28 |
| Ni | 77 | 71 | 111 | 47 | 85 | 65 | 94 | 42 | 25 |
| V | 309 | 329 | 307 | 393 | 305 | 405 | 298 | 419 | 220 |
| Cr | 222 | 253 | 262 | 144 | 187 | 177 | 212 | 97 | 32 |
| CIPW NORM | | | | | | | | | |
| Q | | | | 0.52 | | | | 1.40 | 2.52 |
| Or | 4.37 | 3.78 | 4.08 | 5.67 | 4.85 | 5.13 | 4.13 | 6.22 | 9.83 |
| Ab | 18.53 | 19.55 | 15.99 | 18.70 | 19.80 | 18.86 | 18.94 | 18.74 | 18.83 |
| An | 27.80 | 26.90 | 29.34 | 22.09 | 26.59 | 24.01 | 28.40 | 20.69 | 17.48 |
| Di | 14.18 | 16.65 | 11.77 | 17.43 | 14.59 | 17.44 | 13.99 | 17.60 | 12.88 |
| Hy | 20.18 | 18.07 | 25.35 | 24.17 | 18.72 | 21.93 | 18.34 | 24.18 | 24.77 |
| Ol | 5.40 | 6.14 | 3.02 | | 5.94 | 2.55 | 7.69 | | |
| Mt | 2.72 | 2.64 | 2.77 | 2.98 | 2.62 | 2.97 | 2.70 | 3.17 | 3.26 |
| Il | 4.67 | 4.31 | 4.94 | 5.87 | 4.39 | 5.80 | 4.59 | 6.43 | 6.70 |
| Ap | 1.09 | 0.83 | 1.11 | 1.34 | 1.02 | 1.31 | 1.23 | 1.58 | 3.74 |

Continued table III.

| | 41131 | 41132 | 41147 | 41155 | 41156 | 41166 | 41167 | 41191 | 41192 |
|---|---|---|---|---|---|---|---|---|---|
| $SiO_2$ | 47.48 | 48.24 | 48.21 | 47.78 | 47.84 | 47.92 | 48.88 | 47.71 | 48.34 |
| $TiO_2$ | 2.25 | 2.45 | 2.85 | 2.03 | 2.25 | 1.90 | 2.41 | 2.10 | 2.84 |
| $Al_2O_3$ | 14.95 | 14.71 | 12.74 | 15.56 | 14.99 | 15.70 | 14.43 | 15.47 | 14.10 |
| $Fe_2O_3$ | 3.22 | 1.85 | 2.88 | 1.78 | 2.25 | 1.23 | 2.10 | 2.25 | 2.20 |
| FeO | 11.28 | 12.41 | 13.57 | 11.40 | 11.88 | 11.73 | 11.76 | 11.32 | 12.88 |
| MnO | 0.21 | 0.21 | 0.24 | 0.19 | 0.20 | 0.19 | 0.19 | 0.19 | 0.21 |
| MgO | 7.33 | 6.89 | 6.51 | 7.81 | 7.30 | 8.20 | 6.80 | 7.75 | 6.20 |
| CaO | 10.06 | 9.78 | 9.02 | 10.13 | 9.84 | 9.98 | 10.26 | 9.99 | 9.41 |
| $Na_2O$ | 2.28 | 2.36 | 2.48 | 2.34 | 2.26 | 2.28 | 2.03 | 2.21 | 2.52 |
| $K_2O$ | 0.57 | 0.69 | 1.00 | 0.59 | 0.73 | 0.53 | 0.68 | 0.58 | 0.76 |
| $P_2O_5$ | 0.38 | 0.39 | 0.49 | 0.40 | 0.44 | 0.32 | 0.46 | 0.42 | 0.49 |
| FeO* | 14.18 | 14.08 | 16.16 | 13.00 | 13.91 | 12.84 | 13.65 | 13.35 | 14.86 |
| FeO*/MgO | 1.93 | 2.04 | 2.48 | 1.66 | 1.90 | 1.57 | 2.01 | 1.72 | 2.40 |
| $Fe_2O_3$/FeO | 0.29 | 0.15 | 0.21 | 0.16 | 0.19 | 0.10 | 0.18 | 0.20 | 0.17 |
| $H_2O$ | 0.66 | 0.99 | 0.62 | 0.90 | 1.35 | 0.62 | 1.28 | 0.44 | 1.43 |
| | | | | | | | | | |
| Rb | 16 | 21 | 30 | 18 | 22 | 12 | 21 | 15 | 19 |
| Ba | 191 | 227 | 354 | 220 | 226 | 339 | 217 | 227 | 276 |
| Sr | 153 | 194 | 184 | 164 | 141 | 177 | 143 | 173 | 190 |
| La | 13 | 8 | 13 | 8 | 12 | 8 | 12 | 8 | 10 |
| Y | 47 | 46 | 57 | 43 | 49 | 35 | 49 | 43 | 52 |
| U | 0.393 | 0.459 | 0.686 | 0.383 | 0.415 | 0.308 | 0.555 | 0.396 | 0.526 |
| Th | <2 | <2 | <2 | <2 | <2 | <2 | 4 | 2 | 5 |
| Zr | 192 | 210 | 237 | 181 | 216 | 156 | 209 | 188 | 251 |
| Nb | 8.2 | 13 | 12 | 10 | 11 | 9.1 | 10 | 9.6 | 14 |
| Ni | 103 | 71 | 73 | 109 | 90 | 118 | 72 | 108 | 70 |
| V | 321 | 315 | 378 | 285 | 308 | 279 | 347 | 277 | 359 |
| Cr | 196 | 213 | 73 | 272 | 239 | 302 | 240 | 227 | 189 |

CIPW NORM

| | | | | | | | | | |
|---|---|---|---|---|---|---|---|---|---|
| Q | | | | | | | 0.18 | | |
| Or | 3.37 | 4.10 | 5.92 | 3.50 | 4.30 | 3.13 | 4.00 | 3.43 | 4.48 |
| Ab | 19.32 | 20.01 | 21.01 | 19.79 | 19.16 | 19.29 | 17.18 | 18.74 | 21.31 |
| An | 28.91 | 27.47 | 20.67 | 30.20 | 28.61 | 31.04 | 28.27 | 30.59 | 24.95 |
| Di | 15.36 | 15.30 | 17.44 | 14.34 | 14.32 | 13.46 | 16.22 | 13.37 | 15.46 |
| Hy | 15.10 | 18.39 | 18.55 | 13.60 | 16.95 | 15.03 | 25.89 | 16.92 | 20.25 |
| Ol | 10.06 | 6.46 | 6.75 | 11.30 | 8.69 | 11.25 | | 9.42 | 4.09 |
| Mt | 2.72 | 2.70 | 3.10 | 2.49 | 2.67 | 2.46 | 2.62 | 2.56 | 2.85 |
| Il | 4.28 | 4.66 | 5.42 | 3.85 | 4.28 | 3.61 | 4.58 | 4.00 | 5.49 |
| Ap | 0.88 | 0.91 | 1.14 | 0.93 | 1.03 | 0.74 | 1.08 | 0.98 | 1.12 |

Table IV. E-W profile across a 10 m wide Koster dyke from sector I. Oxides in weight %, elements in ppm.

| | 41135 | 41136 | 41137 | 41138 | 41139 | 41140 | 41141 | 41142 | 41143 | 41144 | 41145 | 41146 |
|---|---|---|---|---|---|---|---|---|---|---|---|---|
| $SiO_2$ | 49.50 | 49.15 | 49.21 | 49.32 | 49.40 | 49.33 | 49.60 | 49.46 | 49.51 | 49.34 | 49.07 | 49.14 |
| $TiO_2$ | 2.10 | 1.99 | 1.97 | 1.91 | 1.91 | 1.95 | 1.77 | 1.89 | 1.91 | 1.91 | 2.10 | 1.95 |
| $Al_2O_3$ | 14.78 | 14.97 | 14.03 | 14.04 | 13.78 | 13.61 | 13.94 | 13.63 | 13.54 | 13.88 | 13.58 | 14.93 |
| $Fe_2O_3$ | 1.39 | 1.75 | 3.14 | 3.05 | 3.31 | 3.31 | 2.88 | 3.38 | 3.43 | 3.30 | 3.45 | 1.50 |
| FeO | 12.00 | 11.59 | 11.22 | 11.13 | 10.93 | 11.05 | 10.69 | 10.82 | 10.84 | 10.90 | 11.57 | 11.90 |
| MnO | 0.20 | 0.20 | 0.22 | 0.21 | 0.22 | 0.22 | 0.21 | 0.21 | 0.22 | 0.22 | 0.22 | 0.20 |
| MgO | 6.67 | 6.65 | 6.60 | 6.69 | 6.90 | 6.87 | 7.15 | 6.95 | 6.90 | 6.78 | 6.43 | 7.05 |
| CaO | 9.94 | 9.99 | 10.27 | 10.34 | 10.38 | 10.34 | 10.56 | 10.42 | 10.38 | 10.35 | 10.24 | 9.88 |
| $Na_2O$ | 2.22 | 2.60 | 2.53 | 2.55 | 2.44 | 2.58 | 2.51 | 2.50 | 2.51 | 2.58 | 2.51 | 2.26 |
| $K_2O$ | 0.83 | 0.78 | 0.53 | 0.50 | 0.49 | 0.50 | 0.46 | 0.49 | 0.50 | 0.50 | 0.54 | 0.82 |
| $P_2O_5$ | 0.38 | 0.35 | 0.27 | 0.26 | 0.25 | 0.25 | 0.23 | 0.25 | 0.25 | 0.26 | 0.30 | 0.36 |
| FeO* | 13.35 | 13.17 | 14.05 | 13.88 | 13.91 | 14.03 | 13.28 | 13.86 | 13.93 | 13.87 | 14.68 | 13.25 |
| FeO*/MgO | 1.99 | 1.98 | 2.13 | 2.07 | 2.02 | 2.04 | 1.86 | 1.99 | 2.02 | 2.05 | 2.28 | 1.88 |
| $Fe_2O_3$/FeO | 0.12 | 0.15 | 0.28 | 0.27 | 0.30 | 0.30 | 0.27 | 0.31 | 0.32 | 0.30 | 0.30 | 0.13 |
| $H_2O$ | 0.68 | 0.67 | 0.48 | 0.44 | 0.44 | 0.26 | 0.34 | 0.56 | 0.65 | 0.48 | 0.46 | 0.56 |
| Rb | 33 | 30 | 10 | 90 | 9.1 | 9.4 | 7.6 | 10 | 95 | 8.9 | 11 | 32 |
| Ba | 229 | 366 | 232 | 384 | 217 | 226 | 215 | 382 | 223 | 373 | 248 | 200 |
| Sr | 142 | 145 | 193 | 189 | 185 | 186 | 186 | 182 | 186 | 187 | 192 | 139 |
| La | 11 | 16 | 2 | 11 | 7 | 8 | 4 | 5 | 6 | 3 | 4 | 13 |
| Y | 51 | 50 | 44 | 41 | 41 | 42 | 39 | 41 | 42 | 41 | 45 | 47 |
| U | 0.857 | 0.725 | 0.202 | 0.187 | | 0.197 | 0.178 | 0.182 | 0.201 | 0.191 | 0.218 | 0.784 |
| Th | <2 | 3 | <2 | <2 | <2 | <2 | <2 | <2 | <2 | <2 | <2 | <2 |
| Zr | 225 | 217 | 140 | 132 | 129 | 133 | 120 | 128 | 129 | 132 | 147 | 206 |
| Nb | 10 | 9.1 | 6.0 | 3.6 | 4.7 | 5.3 | 3.8 | 5.1 | 5.0 | 4.6 | 5.3 | 9.3 |
| Ni | 87 | 86 | 71 | 68 | 69 | 73 | 75 | 69 | 67 | 67 | 54 | 95 |
| V | 311 | 302 | 421 | 406 | 418 | 433 | 392 | 425 | 431 | 408 | 438 | 290 |
| Cr | 218 | 168 | 148 | 154 | 168 | 156 | 203 | 170 | 163 | 167 | 122 | 206 |

Table V. Mean Koster dyke compositions. Based on analyses in Table II, VI, VII and VIII. Oxides in weight %, elements in ppm.

| | Sector I | | Sector II | | Sector III >2m | | Sector III <2m | |
|---|---|---|---|---|---|---|---|---|
| | $\bar{x}$ | s | $\bar{x}$ | s | $\bar{x}$ | s | $\bar{x}$ | s |
| $SiO_2$ | 48.22 | 0.61 | 48.15 | 0.83 | 48.06 | 0.90 | 47.41 | 1.56 |
| $TiO_2$ | 2.52 | 0.41 | 2.42 | 0.35 | 2.34 | 0.40 | 2.21 | 0.37 |
| $Al_2O_3$ | 14.41 | 0.99 | 14.69 | 0.86 | 14.84 | 0.86 | 14.87 | 0.69 |
| $Fe_2O_3$ | 2.46 | 0.57 | 2.93 | 0.50 | 2.46 | 0.76 | 2.30 | 0.45 |
| FeO | 12.11 | 0.84 | 11.54 | 0.77 | 11.97 | 0.69 | 11.82 | 0.7978 |
| MnO | 0.21 | 0.02 | 0.21 | 0.01 | 0.21 | 0.02 | 0.20 | 0.03 |
| MgO | 6.88 | 0.75 | 6.78 | 0.71 | 6.95 | 0.80 | 7.16 | 0.70 |
| CaO | 9.76 | 0.33 | 9.44 | 0.52 | 9.52 | 0.43 | 9.87 | 0.79 |
| $Na_2O$ | 2.27 | 0.44 | 2.48 | 0.24 | 2.42 | 0.22 | 2.12 | 0.47 |
| $K_2O$ | 0.74 | 0.15 | 0.82 | 0.18 | 0.84 | 0.27 | 1.53 | 0.83 |
| $P_2O_5$ | 0.47 | 0.09 | 0.40 | 0.10 | 0.42 | 0.08 | 0.39 | 0.09 |
| FeO* | 14.91 | 0.99 | 14.33 | 0.75 | 14.18 | 0.93 | 13.88 | 0.90 |
| FeO*/MgO | 2.13 | 0.40 | 2.14 | 0.30 | 2.07 | 0.39 | 1.96 | 0.31 |
| $Fe_2O_3/FeO$ | 0.20 | 0.05 | 0.27 | 0.04 | 0.21 | 0.06 | 0.20 | 0.04 |
| $H_2O$ | 0.85 | 0.35 | 1.56 | 0.45 | 1.94 | 0.34 | 1.97 | 0.43 |
| Rb | 24 | 8.6 | 30 | 9.5 | 31 | 19.4 | 75 | 57.9 |
| Ba | 303 | 116.8 | 292 | 121.1 | 235 | 87.0 | 245 | 109.6 |
| Sr | 162 | 19.7 | 167 | 21.0 | 169 | 14.1 | 139 | 29.8 |
| La | 13 | 4.9 | 13 | 5.7 | 12 | 5.3 | 11 | 6.5 |
| Y | 51 | 9.0 | 47 | 9.9 | 47 | 6.4 | 46 | 6.9 |
| U | 0.5650 | 0.2193 | 0.5871 | 0.3450 | 0.6617 | 0.1590 | 0.6201 | 0.2908 |
| Zr | 224 | 40.7 | 202 | 54.9 | 203 | 34.3 | 182 | 57.0 |
| Nb | 11.6 | 2.2 | 10.5 | 3.4 | 10.5 | 2.0 | 10.8 | 4.1 |
| Ni | 83 | 22.2 | 83 | 25.1 | 86 | 24.7 | 86 | 23.7 |
| V | 331 | 44.6 | 340 | 50.6 | 315 | 54.9 | 327 | 39.6 |
| Cr | 206 | 59.7 | 207 | 74.7 | 205 | 80.8 | 201 | 57.8 |

Table VI. Koster dykes from sector II. Oxides in weight %, elements in ppm.

| | 41104 | 41105 | 41106 | 41109 | 41149 | 41153 | 41154 | LS3 | LS4 | LS5 | LS6 | LS7 |
|---|---|---|---|---|---|---|---|---|---|---|---|---|
| $SiO_2$ | 47.63 | 49.48 | 48.79 | 47.80 | 48.79 | 49.01 | 47.15 | 47.52 | 47.44 | 47.67 | 49.22 | 48.16 |
| $TiO_2$ | 1.75 | 2.05 | 2.94 | 2.29 | 2.72 | 3.55 | 2.61 | 2.42 | 2.58 | 2.26 | 2.61 | 1.11 |
| $Al_2O_3$ | 16.03 | 13.72 | 13.71 | 14.93 | 13.51 | 11.86 | 14.93 | 15.13 | 15.34 | 15.48 | 14.16 | 18.16 |
| $Fe_2O_3$ | 2.69 | 3.82 | 3.36 | 2.84 | 3.28 | 2.45 | 2.41 | 2.62 | 3.37 | 3.28 | 2.91 | 2.11 |
| FeO | 10.26 | 10.97 | 12.22 | 11.32 | 12.33 | 11.64 | 12.47 | 11.81 | 11.92 | 10.46 | 11.75 | 8.73 |
| MnO | 0.18 | 0.21 | 0.20 | 0.20 | 0.22 | 0.26 | 0.21 | 0.20 | 0.22 | 0.21 | 0.22 | 0.17 |
| MgO | 8.29 | 6.39 | 6.20 | 7.41 | 5.88 | 3.90 | 6.95 | 6.86 | 6.50 | 7.07 | 6.23 | 8.03 |
| CaO | 9.99 | 10.20 | 8.60 | 10.10 | 9.12 | 8.36 | 9.30 | 9.48 | 9.08 | 9.53 | 9.04 | 10.53 |
| $Na_2O$ | 2.33 | 2.31 | 2.27 | 2.00 | 2.71 | 2.51 | 2.62 | 2.62 | 2.53 | 2.77 | 2.61 | 2.61 |
| $K_2O$ | 0.58 | 0.56 | 1.14 | 0.73 | 0.94 | 1.67 | 0.92 | 0.91 | 0.67 | 0.92 | 0.80 | 0.30 |
| $P_2O_5$ | 0.28 | 0.27 | 0.58 | 0.39 | 0.48 | 1.80 | 0.43 | 0.41 | 0.34 | 0.37 | 0.49 | 0.10 |
| FeO* | 12.68 | 14.41 | 15.24 | 13.88 | 15.28 | 16.85 | 14.64 | 14.17 | 14.95 | 13.41 | 14.37 | 10.63 |
| FeO*/MgO | 1.53 | 2.25 | 2.46 | 1.87 | 2.60 | 4.32 | 2.11 | 2.07 | 2.30 | 1.90 | 2.31 | 1.32 |
| $Fe_2O_3$/FeO | 0.26 | 0.35 | 0.27 | 0.25 | 0.27 | 0.17 | 0.19 | 0.22 | 0.28 | 0.31 | 0.25 | 0.24 |
| $H_2O$ | 1.55 | 0.81 | 0.98 | 1.53 | 1.31 | 1.67 | 1.45 | 1.90 | 2.2 | 2.0 | 1.9 | 1.9 |
| Rb | 23 | 16 | 50 | 28 | 29 | 72 | 32 | 37 | 21 | 29 | 35 | 7.5 |
| Ba | 123 | 378 | 334 | 336 | 499 | 921 | 323 | 382 | 150 | 226 | 166 | 126 |
| Sr | 144 | 178 | 156 | 155 | 193 | 132 | 200 | 162 | 186 | 144 | 148 | 182 |
| La | 10 | 5 | 26 | 13 | 13 | 65 | 17 | 16 | 11 | 8 | 13 | <2 |
| Y | 33 | 42 | 64 | 42 | 56 | 148 | 48 | 47 | 50 | 32 | 52 | 22 |
| U | 0.302 | 0.219 | 1.29 | 0.441 | 0.701 | 2.41 | 0.478 | 0.523 | 0.909 | 0.437 | 0.968 | 0.190 |
| Th | <2 | <2 | <2 | <2 | <2 | 8 | <2 | <2 | 3 | <2 | <2 | <2 |
| Zr | 128 | 140 | 309 | 182 | 233 | 1080 | 235 | 205 | 222 | 147 | 223 | 62 |
| Nb | 6.2 | 5.3 | 16 | 8.8 | 12 | 33 | 14 | 12 | 10 | 8.6 | 12 | 1.2 |
| Ni | 133 | 66 | 79 | 88 | 58 | 22 | 92 | 81 | 101 | 89 | 41 | 99 |
| V | 267 | 443 | 321 | 330 | 401 | 178 | 325 | 327 | 303 | 319 | 366 | 263 |
| Cr | 274 | 153 | 191 | 288 | 70 | 6 | 267 | 243 | 105 | 245 | 229 | 156 |

Table VII. Koster dykes >2 m from sector III. Oxides in weight %, elements in ppm.

| | LS1 | 41107 | 41108 | 41179 | 51701 | 51703 | 51749 | 51751 | 51753 | 51754 | LS2 | LS8 | LS9 |
|---|---|---|---|---|---|---|---|---|---|---|---|---|---|
| $SiO_2$ | 47.15 | 49.53 | 48.11 | 47.66 | 47.71 | 47.17 | 49.07 | 46.91 | 47.75 | 47.75 | 49.70 | 48.57 | 47.69 |
| $TiO_2$ | 1.65 | 2.90 | 2.33 | 2.43 | 2.40 | 1.97 | 2.17 | 2.78 | 2.30 | 2.04 | 1.99 | 2.44 | 3.08 |
| $Al_2O_3$ | 16.55 | 13.21 | 15.67 | 15.38 | 14.91 | 15.57 | 14.28 | 14.70 | 15.05 | 14.79 | 14.38 | 14.66 | 13.75 |
| $Fe_2O_3$ | 1.67 | 3.96 | 2.79 | 1.96 | 2.01 | 1.63 | 1.94 | 2.16 | 2.22 | 2.66 | 2.98 | 2.14 | 3.87 |
| FeO | 11.14 | 12.11 | 11.36 | 12.35 | 12.06 | 11.91 | 12.71 | 13.51 | 12.01 | 11.42 | 10.92 | 11.81 | 12.29 |
| MnO | 0.20 | 0.23 | 0.20 | 0.21 | 0.20 | 0.20 | 0.21 | 0.23 | 0.20 | 0.20 | 0.22 | 0.20 | 0.26 |
| MgO | 7.81 | 5.12 | 7.39 | 7.64 | 7.32 | 7.86 | 6.18 | 6.71 | 7.68 | 7.31 | 6.48 | 6.72 | 6.35 |
| CaO | 9.99 | 8.88 | 9.77 | 9.51 | 10.09 | 10.24 | 9.52 | 9.19 | 8.87 | 9.19 | 9.45 | 9.78 | 9.32 |
| $Na_2O$ | 2.60 | 2.65 | 2.03 | 2.14 | 2.28 | 2.52 | 2.47 | 2.67 | 2.41 | 2.74 | 2.27 | 2.44 | 2.27 |
| $K_2O$ | 1.04 | 0.87 | 0.51 | 1.05 | 0.57 | 0.59 | 0.70 | 0.68 | 1.11 | 1.49 | 0.85 | 0.81 | 0.68 |
| $P_2O_5$ | 0.23 | 0.54 | 0.43 | 0.45 | 0.44 | 0.33 | 0.42 | 0.46 | 0.39 | 0.40 | 0.47 | 0.48 | 0.45 |
| FeO* | 12.64 | 15.67 | 13.87 | 14.11 | 13.87 | 13.38 | 14.46 | 15.45 | 14.01 | 13.81 | 13.60 | 13.74 | 15.77 |
| FeO*/MgO | 1.62 | 3.06 | 1.88 | 1.85 | 1.89 | 1.70 | 2.34 | 2.30 | 1.82 | 1.89 | 2.10 | 2.03 | 2.48 |
| $Fe_2O_3$/FeO | 0.15 | 0.33 | 0.25 | 0.16 | 0.17 | 0.14 | 0.15 | 0.16 | 0.18 | 0.23 | 0.27 | 0.18 | 0.31 |
| $H_2O$ | 2.4 | 1.69 | 1.74 | 2.38 | 2.33 | 1.77 | 1.24 | 1.66 | 1.94 | 2.15 | 1.80 | 2.0 | 2.1 |
| | | | | | | | | | | | | | |
| Rb | 53 | 15 | 11 | 43 | 11 | 17 | 24 | 15 | 59 | 69 | 31 | 33 | 22 |
| Ba | 155 | 228 | 136 | 213 | 310 | 312 | 304 | 141 | 177 | 365 | 150 | 374 | 189 |
| Sr | 173 | 199 | 161 | 194 | 162 | 162 | 170 | 164 | 176 | 163 | 154 | 151 | 165 |
| La | <2 | 16 | 19 | 12 | 3 | 11 | 14 | 18 | 13 | 9 | 12 | 15 | 14 |
| Y | 36 | 56 | 45 | 45 | 44 | 40 | 53 | 43 | 42 | 42 | 53 | 49 | 56 |
| U | | 0.713 | 0.482 | 0.875 | 0.629 | 0.376 | 0.777 | 0.709 | 0.636 | 0.624 | 0.953 | 0.585 | 0.581 |
| Th | 2 | <2 | 2 | <2 | <2 | <2 | 2 | 2 | <2 | <2 | <2 | 3 | <2 |
| Zr | 127 | 230 | 229 | 206 | 197 | 166 | 233 | 219 | 179 | 178 | 200 | 213 | 259 |
| Nb | 7.0 | 9.7 | 10 | 11 | 11 | 8.9 | 9.7 | 14 | 11 | 11 | 7.7 | 11 | 14 |
| Ni | 90 | 43 | 79 | 134 | 87 | 99 | 68 | 90 | 127 | 90 | 73 | 73 | 63 |
| V | 298 | 460 | 300 | 308 | 308 | 296 | 280 | 334 | 272 | 291 | 239 | 335 | 378 |
| Cr | 111 | 65 | 294 | 281 | 266 | 164 | 119 | 206 | 313 | 273 | 135 | 249 | 188 |

Table VIII. Koster dykes ≤2 m from sector III. Oxides in weight %, elements in ppm.

| | 41178 | 41181 | 41183 | 41184 | 41186 | 51702 | 51704 | 51748 | 51752 | 51755 |
|---|---|---|---|---|---|---|---|---|---|---|
| $SiO_2$ | 44.50 | 47.55 | 47.00 | 46.02 | 47.77 | 46.90 | 47.43 | 49.39 | 50.05 | 47.44 |
| $TiO_2$ | 2.77 | 2.22 | 2.38 | 2.42 | 1.85 | 1.64 | 2.00 | 2.09 | 2.74 | 2.03 |
| $Al_2O_3$ | 15.23 | 15.13 | 14.76 | 14.77 | 15.26 | 15.52 | 15.31 | 14.57 | 13.10 | 15.04 |
| $Fe_2O_3$ | 2.15 | 2.28 | 3.06 | 2.62 | 1.65 | 1.79 | 1.90 | 2.28 | 2.51 | 2.79 |
| FeO | 13.09 | 11.01 | 11.14 | 12.46 | 11.23 | 11.17 | 11.98 | 12.08 | 12.88 | 11.06 |
| MnO | 0.23 | 0.21 | 0.19 | 0.15 | 0.18 | 0.20 | 0.20 | 0.21 | 0.24 | 0.22 |
| MgO | 7.47 | 7.36 | 6.77 | 7.20 | 7.92 | 7.78 | 7.84 | 6.31 | 5.74 | 7.27 |
| CaO | 11.47 | 9.43 | 10.38 | 9.69 | 10.36 | 10.32 | 9.67 | 9.46 | 8.64 | 9.27 |
| $Na_2O$ | 1.61 | 1.86 | 2.04 | 1.18 | 1.97 | 2.49 | 2.57 | 2.52 | 2.33 | 2.59 |
| $K_2O$ | 1.04 | 2.55 | 1.83 | 2.97 | 1.53 | 0.61 | 0.75 | 0.64 | 1.27 | 2.15 |
| $P_2O_5$ | 0.45 | 0.40 | 0.43 | 0.47 | 0.32 | 0.20 | 0.35 | 0.43 | 0.50 | 0.33 |
| FeO* | 15.03 | 13.06 | 13.89 | 14.82 | 12.72 | 12.78 | 13.69 | 14.13 | 15.14 | 13.57 |
| FeO*/MgO | 2.01 | 1.77 | 2.05 | 2.06 | 1.61 | 1.64 | 1.75 | 2.24 | 2.64 | 1.87 |
| $Fe_2O_3$/FeO | 0.16 | 0.21 | 0.27 | 0.21 | 0.15 | 0.16 | 0.16 | 0.19 | 0.19 | 0.25 |
| $H_2O$ | | 2.72 | 1.76 | 2.15 | 2.51 | 1.71 | 2.04 | 1.47 | 1.80 | 1.54 |
| | | | | | | | | | | |
| Rb | 31 | 161 | 80 | 172 | 72 | 23 | 26 | 14 | 49 | 119 |
| Ba | 359 | 437 | 363 | 126 | 293 | 189 | 168 | 153 | 205 | 152 |
| Sr | 106 | 133 | 162 | 138 | 176 | 169 | 175 | 116 | 112 | 100 |
| La | 13 | 6 | 19 | 12 | 6 | <2 | 6 | 22 | 15 | 9 |
| Y | 53 | 47 | 44 | 46 | 36 | 37 | 41 | 51 | 58 | 46 |
| U | 0.687 | 0.507 | 0.782 | 0.468 | 0.328 | 0.252 | 0.453 | 1.17 | 0.994 | 0.560 |
| Th | 2 | <2 | <2 | <2 | <2 | <2 | <2 | 4 | <2 | <2 |
| Zr | 236 | 187 | 198 | 213 | 128 | 132 | 170 | 233 | 248 | 171 |
| Nb | 21 | 10 | 12 | 11 | 5.9 | 7.3 | 9.1 | 9.5 | 13 | 9.6 |
| Ni | 107 | 99 | 68 | 70 | 114 | 92 | 100 | 81 | 33 | 92 |
| V | 390 | 311 | 325 | 346 | 303 | 327 | 307 | 260 | 389 | 312 |
| Cr | 258 | 257 | 232 | 202 | 290 | 127 | 168 | 115 | 184 | 177 |

Table IX. Samples from profile A, Kattsund dyke. The samples are numbered from west towards east. Oxides in weight %, elements in ppm.

| | 1 | 2 | 3 | 4 | 5 | 6 | 7 | 8 |
|---|---|---|---|---|---|---|---|---|
| $SiO_2$ | 46.30 | 48.89 | 49.03 | 49.42 | 50.75 | 50.98 | 51.23 | 49.31 |
| $TiO_2$ | 0.85 | 1.49 | 1.44 | 1.46 | 2.03 | 1.90 | 1.93 | 1.42 |
| $Al_2O_3$ | 15.13 | 14.99 | 15.03 | 14.74 | 13.60 | 13.31 | 13.66 | 14.83 |
| $Fe_2O_3$ | 3.63 | 2.67 | 2.69 | 3.75 | 4.65 | 3.91 | 3.55 | 2.68 |
| FeO | 12.85 | 10.34 | 9.97 | 9.25 | 9.27 | 10.06 | 10.25 | 10.18 |
| MnO | 0.24 | 0.17 | 0.17 | 0.22 | 0.25 | 0.24 | 0.21 | 0.17 |
| MgO | 9.86 | 7.72 | 7.83 | 7.78 | 6.66 | 6.70 | 6.74 | 7.69 |
| CaO | 6.89 | 9.78 | 9.54 | 9.47 | 8.99 | 9.16 | 8.60 | 9.48 |
| $Na_2O$ | 1.71 | 2.61 | 2.99 | 2.72 | 2.75 | 2.47 | 2.64 | 2.85 |
| $K_2O$ | 2.42 | 1.21 | 1.14 | 1.07 | 0.85 | 1.13 | 0.99 | 1.24 |
| $P_2O_5$ | 0.13 | 0.14 | 0.14 | 0.12 | 0.20 | 0.16 | 0.21 | 0.14 |
| FeO* | 16.12 | 12.74 | 12.39 | 12.63 | 13.46 | 13.31 | 13.45 | 12.59 |
| FeO*/MgO | 1.63 | 1.65 | 1.58 | 1.62 | 2.02 | 1.99 | 1.99 | 1.64 |
| $Fe_2O_3$/FeO | 0.28 | 0.26 | 0.26 | 0.41 | 0.50 | 0.39 | 0.35 | 0.26 |
| $H_2O$ | 3.17 | 2.02 | 1.80 | 2.15 | 1.80 | 1.73 | 1.85 | 2.07 |
| Rb | 190 | 61 | 61 | 57 | 41 | 60 | 45 | 62 |
| Ba | 546 | 357 | 369 | 351 | 279 | 372 | 283 | 408 |
| Sr | 131 | 229 | 252 | 257 | 244 | 246 | 201 | 286 |
| La | 5 | 1 | <1 | 4 | 5 | 4 | 2 | 2 |
| Y | 34 | 28 | 29 | 28 | 41 | 34 | 38 | 27 |
| U | 0.485 | 0.149 | 0.118 | 0.120 | 0.175 | 0.240 | 0.151 | 0.151 |
| Zr | 51 | 56 | 63 | 43 | 79 | 61 | 93 | 60 |
| Nb | 4.4 | 2.4 | 1.9 | 0.6 | 1.6 | 1.4 | 2.5 | 2.8 |
| Ni | 166 | 115 | 118 | 119 | 69 | 71 | 67 | 116 |
| V | 325 | 385 | 406 | 345 | 432 | 470 | 491 | 401 |
| Cr | 570 | 206 | 216 | 228 | 120 | 139 | 116 | 201 |
| Cl | 1274 | 436 | 471 | 264 | 405 | 345 | 462 | 337 |
| S | 238 | 189 | 64 | 105 | 819 | 72 | 2274 | 51 |

Table X. Samples from profile B, Kattsund dyke. The samples are numbered from west towards east. Oxides in weight %, elements in ppm.

| | 1 | 2 | 3 | 4 | 5 | 6 | 7 |
|---|---|---|---|---|---|---|---|
| $SiO_2$ | 51.11 | 51.12 | 49.70 | 49.40 | 49.03 | 49.13 | 52.67 |
| $TiO_2$ | 1.75 | 1.84 | 2.86 | 2.57 | 2.58 | 2.74 | 2.02 |
| $Al_2O_3$ | 13.51 | 13.48 | 12.48 | 12.73 | 12.72 | 12.54 | 14.34 |
| $Fe_2O_3$ | 3.51 | 3.88 | 4.08 | 4.38 | 4.22 | 4.45 | 2.05 |
| FeO | 10.25 | 10.24 | 12.57 | 12.00 | 12.18 | 12.37 | 14.82 |
| MnO | 0.17 | 0.17 | 0.22 | 0.20 | 0.20 | 0.20 | 0.44 |
| MgO | 6.43 | 6.06 | 5.53 | 5.80 | 6.11 | 5.69 | 6.66 |
| CaO | 9.81 | 9.86 | 9.10 | 9.32 | 9.40 | 9.40 | 3.76 |
| $Na_2O$ | 2.57 | 2.39 | 2.35 | 2.52 | 2.29 | 2.29 | 1.92 |
| $K_2O$ | 0.71 | 0.76 | 0.75 | 0.79 | 0.98 | 0.87 | 1.10 |
| $P_2O_5$ | 0.18 | 0.19 | 0.34 | 0.30 | 0.29 | 0.33 | 0.22 |
| FeO* | 13.41 | 13.73 | 16.24 | 15.94 | 15.98 | 16.38 | 16.67 |
| FeO*/MgO | 2.09 | 2.27 | 2.94 | 2.75 | 2.61 | 2.88 | 2.50 |
| $Fe_2O_3$/Feo | 0.34 | 0.38 | 0.32 | 0.36 | 0.35 | 0.36 | 0.14 |
| $H_2O$ | 1.37 | 1.48 | 1.30 | 1.53 | 1.40 | 1.51 | 5.07 |
| Rb | 21 | 22 | 24 | 30 | 46 | 30 | 65 |
| Ba | 231 | 235 | 372 | 319 | 515 | 171 | 293 |
| Sr | 175 | 171 | 142 | 124 | 139 | 142 | 148 |
| La | 3 | 8 | 3 | 16 | 9 | 7 | 1 |
| Y | 35 | 38 | 50 | 48 | 48 | 50 | 32 |
| U | 0.281 | 0.270 | 0.309 | 0.318 | 0.474 | 0.303 | 0.479 |
| Zr | 85 | 96 | 148 | 131 | 130 | 136 | 94 |
| Nb | 3.9 | 3.4 | 3.9 | 4.2 | 3.7 | 3.9 | 3.2 |
| Ni | 52 | 46 | 50 | 57 | 59 | 32 | 52 |
| V | 481 | 461 | 617 | 580 | 590 | 614 | 553 |
| Cr | 100 | 89 | 73 | 117 | 127 | 90 | 87 |
| Cl | 613 | 852 | 799 | 1121 | 908 | 477 | 129 |
| S | 64 | 696 | 394 | 175 | 76 | 1957 | 9171 |

Table XI. Samples from profile C, Kattsund dyke. The samples are numbered from west towards east. Oxides in %, elements in ppm.

| | 1 | 2 | 3 | 4 | 5 | 6 | 7 | 8 | 9 |
|---|---|---|---|---|---|---|---|---|---|
| $SiO_2$ | 49.53 | 49.83 | 49.59 | 49.00 | 49.60 | 49.79 | 49.18 | 49.45 | 48.16 |
| $TiO_2$ | 3.01 | 2.93 | 2.95 | 2.96 | 2.84 | 2.09 | 2.88 | 2.87 | 2.97 |
| $Al_2O_3$ | 12.05 | 11.96 | 12.08 | 12.12 | 12.12 | 12.57 | 12.12 | 12.19 | 12.45 |
| $Fe_2O_3$ | 5.47 | 5.22 | 5.43 | 5.12 | 5.33 | 4.32 | 5.61 | 4.53 | 4.48 |
| FeO | 12.06 | 12.22 | 12.11 | 12.55 | 12.03 | 11.94 | 12.01 | 12.77 | 13.41 |
| MnO | 0.29 | 0.26 | 0.28 | 0.29 | 0.28 | 0.19 | 0.30 | 0.22 | 0.20 |
| MgO | 4.93 | 4.93 | 5.00 | 5.22 | 5.23 | 5.58 | 5.29 | 5.09 | 5.42 |
| CaO | 8.43 | 8.62 | 8.75 | 9.06 | 8.89 | 9.70 | 8.90 | 8.82 | 8.33 |
| $Na_2O$ | 1.83 | 1.85 | 2.15 | 2.15 | 2.20 | 2.33 | 2.28 | 2.05 | 1.81 |
| $K_2O$ | 2.07 | 1.81 | 1.28 | 1.19 | 1.13 | 1.26 | 1.08 | 1.66 | 2.42 |
| $P_2O_5$ | 0.37 | 0.37 | 0.39 | 0.36 | 0.37 | 0.20 | 0.35 | 0.35 | 0.37 |
| FeO* | 16.98 | 16.92 | 17.00 | 17.16 | 16.83 | 15.83 | 17.06 | 16.85 | 17.44 |
| FeO*/MgO | 3.44 | 3.43 | 3.40 | 3.29 | 3.22 | 2.84 | 3.22 | 3.31 | 3.22 |
| $Fe_2O_3$/FeO | 0.45 | 0.43 | 0.45 | 0.41 | 0.44 | 0.36 | 0.47 | 0.35 | 0.33 |
| $H_2O$ | 1.91 | 1.52 | 1.41 | 1.41 | 1.00 | 0.32 | 1.27 | 1.46 | 1.66 |
| Rb | 126 | 99 | 49 | 44 | 36 | 42 | 37 | 79 | 160 |
| Ba | 403 | 351 | 273 | 233 | 242 | 229 | 245 | 285 | 485 |
| Sr | 100 | 103 | 133 | 129 | 133 | 137 | 138 | 127 | 96 |
| La | 14 | 11 | 9 | 9 | 9 | 3 | 9 | 21 | 13 |
| Y | 70 | 63 | 61 | 60 | 57 | 44 | 55 | 54 | 60 |
| U | 0.976 | 0.699 | 0.539 | 0.512 | 0.488 | 0.531 | 0.504 | 0.474 | 0.684 |
| Zr | 135 | 138 | 134 | 125 | 127 | 127 | 123 | 150 | 161 |
| Nb | 4.9 | 5.7 | 4.9 | 4.9 | 4.3 | 4.1 | 3.6 | 4.8 | 5.5 |
| Ni | 28 | 30 | 31 | 32 | 35 | 38 | 31 | 32 | 23 |
| V | 565 | 568 | 556 | 591 | 569 | 574 | 564 | 620 | 662 |
| Cr | 46 | 50 | 55 | 55 | 62 | 60 | 63 | 54 | 42 |
| Cl | 1258 | 1180 | 732 | 904 | 1043 | 1420 | 1130 | 665 | 2934 |
| S | 1396 | 1833 | 1960 | 1519 | 1737 | 52 | 2637 | 2080 | 173 |

Table XII. Paired samples (see text p. 33). Oxides in weight %, elements in ppm. C = sample from layer centre, M = sample from layer margin.
$M_1$—$M_9$ pairs from the Kattsund dykes
$M_{10}$—$M_{13}$ pairs from the Koster dykes
$G_1$—$G_8$ pairs from the Sandbukta gneiss
$I_1$—$I_3$ pairs of interior dykes within multiple Kattsund dykes.

| | $M_1$ | | $M_2$ | | $M_3$ | | $M_4$ | | $M_5$ | |
|---|---|---|---|---|---|---|---|---|---|---|
| | C | M | C | M | C | M | C | M | C | M |
| SiO2 | 49.87 | 50.13 | 50.29 | 47.74 | 48.84 | 50.20 | 48.19 | 49.02 | 49.42 | 46.30 |
| TiO2 | 2.54 | 2.77 | 2.02 | 2.09 | 2.82 | 1.99 | 2.92 | 3.14 | 1.46 | 0.85 |
| Al2O3 | 12.44 | 12.19 | 12.98 | 14.45 | 12.52 | 13.01 | 12.51 | 12.44 | 14.74 | 15.13 |
| Fe2O3 | 5.06 | 4.59 | 3.98 | 3.67 | 4.68 | 3.92 | 4.38 | 3.74 | 3.75 | 3.63 |
| FeO | 11.81 | 12.86 | 11.02 | 13.18 | 12.09 | 11.17 | 12.92 | 12.82 | 9.25 | 12.85 |
| MnO | 0.20 | 0.19 | 0.19 | 0.20 | 0.20 | 0.19 | 0.20 | 0.14 | 0.22 | 0.24 |
| MgO | 5.10 | 4.83 | 6.49 | 7.07 | 5.78 | 6.46 | 5.77 | 5.95 | 7.78 | 9.86 |
| CaO | 8.52 | 8.28 | 9.37 | 8.29 | 9.42 | 9.42 | 9.42 | 9.29 | 9.47 | 6.87 |
| Na2O | 2.45 | 2.00 | 2.07 | 1.69 | 2.63 | 2.06 | 2.41 | 0.75 | 2.72 | 1.71 |
| K2O | 1.72 | 1.82 | 1.39 | 1.43 | 0.70 | 1.39 | 0.93 | 2.32 | 1.07 | 2.42 |
| P2O5 | 0.30 | 0.36 | 0.19 | 0.19 | 0.30 | 0.19 | 0.34 | 0.40 | 0.12 | 0.13 |
| FeO* | 16.36 | 16.97 | 16.60 | 16.48 | 16.31 | 14.69 | 16.86 | 16.18 | 12.63 | 16.12 |
| Fe2O3/FeO | 0.43 | 0.36 | 0.36 | 0.28 | 0.39 | 0.35 | 0.34 | 0.29 | 0.41 | 0.26 |
| H2O | 1.98 | 1.86 | 1.44 | 3.66 | 1.06 | 1.72 | 1.42 | 2.28 | 2.15 | 3.17 |
| Rb | 67 | 69 | 65 | 68 | 20 | 63 | 30 | 129 | 57 | 191 |
| Ba | 186 | 285 | 368 | 329 | 221 | 353 | 216 | 342 | 351 | 516 |
| Sr | 140 | 130 | 143 | 140 | 145 | 138 | 146 | 96 | 256 | 132 |
| La | 10 | 10 | 5 | 8 | 6 | 9 | 7 | | 4 | 5 |
| Y | 52 | 59 | 43 | 48 | 53 | 44 | 50 | 57 | 28 | 34 |
| U | 0.525 | 0.542 | 0.523 | 0.495 | 0.493 | 0.524 | 0.427 | 1.38 | 0.120 | 0.485 |
| Zr | 148 | 160 | 112 | 101 | 155 | 109 | 142 | 136 | 43 | 51 |
| Nb | 4.0 | 5.5 | 2.7 | 3.0 | 5.0 | 3.5 | 4.4 | 5.0 | 0.6 | 4.4 |
| Ni | 30 | 23 | 57 | 55 | 54 | 46 | 48 | 31 | 119 | 166 |
| V | 601 | 596 | 515 | 555 | 373 | 508 | 674 | 610 | 345 | 325 |
| Cr | 53 | 16 | 123 | 124 | 116 | 125 | 112 | 65 | 228 | 570 |

| | $M_6$ | | $M_7$ | | $M_8$ | | $M_9$ | | $M_{10}$ | |
|---|---|---|---|---|---|---|---|---|---|---|
| | C | M | C | M | C | M | C | M | C | M |
| SiO2 | 49.60 | 49.53 | 49.60 | 48.16 | 49.03 | 52.67 | 49.86 | 48.46 | 47.17 | 47.43 |
| TiO2 | 2.84 | 3.01 | 2.84 | 2.97 | 2.58 | 2.02 | 2.57 | 3.02 | 1.97 | 2.00 |
| Al2O3 | 12.12 | 12.04 | 12.12 | 12.45 | 12.72 | 14.34 | 12.73 | 12.26 | 15.57 | 15.31 |
| Fe2O3 | 5.33 | 5.47 | 5.33 | 4.48 | 4.22 | 2.05 | 4.03 | 4.50 | 1.63 | 1.90 |
| FeO | 12.03 | 12.06 | 12.03 | 13.41 | 12.18 | 14.79 | 11.99 | 13.00 | 11.91 | 11.98 |
| MnO | 0.28 | 0.29 | 0.28 | 0.20 | 0.20 | 0.44 | 0.19 | 0.20 | 0.20 | 0.20 |
| MgO | 5.23 | 4.93 | 5.23 | 5.40 | 6.11 | 6.66 | 5.65 | 5.38 | 7.86 | 7.84 |
| CaO | 8.89 | 8.43 | 8.89 | 8.33 | 9.40 | 3.78 | 9.16 | 9.50 | 10.24 | 9.67 |
| Na2O | 2.20 | 1.83 | 2.20 | 1.81 | 2.29 | 1.92 | 2.55 | 1.56 | 2.52 | 21.57 |
| K2O | 1.13 | 2.04 | 1.13 | 2.42 | 0.98 | 1.10 | 0.97 | 1.77 | 0.59 | 0.75 |
| P2O5 | 0.37 | 0.37 | 0.37 | 0.37 | 0.29 | 0.22 | 0.30 | 0.34 | 0.33 | 0.35 |
| FeO* | 16.82 | 16.98 | 16.82 | 17.45 | 15.98 | 16.63 | 15.62 | 17.05 | 13.38 | 13.69 |
| Fe2O3/FeO | 0.44 | 0.45 | 0.44 | 0.33 | 0.35 | 0.14 | 0.34 | 0.35 | 0.14 | 0.16 |
| H2O | 1.00 | 1.91 | 1.00 | 1.66 | 1.40 | 5.07 | 1.41 | 2.05 | 1.77 | 2.04 |
| Rb | 37 | 126 | 37 | 160 | 45 | 64 | 28 | 91 | 17 | 26 |
| Ba | 242 | 403 | 242 | 485 | 515 | 293 | 343 | 398 | 312 | 168 |
| Sr | 136 | 100 | 136 | 96 | 137 | 145 | 141 | 92 | 162 | 175 |
| La | 9 | 14 | 9 | 13 | 9 | 1 | 7 | 11 | 11 | 6 |
| Y | 57 | 70 | 57 | 60 | 48 | 32 | 46 | 61 | 40 | 41 |
| U | 0.488 | 0.976 | 0.488 | 0.684 | 0.474 | 0.479 | 0.433 | 0.496 | <2 | <2 |
| Zr | 127 | 135 | 127 | 161 | 130 | 94 | 126 | 179 | 166 | 170 |
| Nb | 4.3 | 4.9 | 4.3 | 5.5 | 3.7 | 3.2 | 4.8 | 5.1 | 8.9 | 9.1 |
| Ni | 35 | 28 | 35 | 23 | 59 | 52 | 35 | 43 | 99 | 100 |
| V | 569 | 565 | 569 | 662 | 590 | 553 | 564 | 656 | 296 | 307 |
| Cr | 62 | 46 | 62 | 42 | 127 | 87 | 93 | 71 | 164 | 168 |

Continued table XII.

| | $M_{11}$ | | $M_{12}$ | | $M_{13}$ | |
|---|---|---|---|---|---|---|
| | C | M | C | M | C | M |
| SiO2 | 47.66 | 44.50 | 49.46 | 46.64 | 48.37 | 48.01 |
| TiO2 | 2.43 | 2.77 | 2.10 | 2.45 | 2.07 | 2.05 |
| Al2O3 | 15.38 | 15.23 | 13.64 | 14.95 | 14.99 | 15.11 |
| Fe2O3 | 1.96 | 2.15 | 1.98 | 1.93 | 1.98 | 2.09 |
| FeO | 12.35 | 13.09 | 11.15 | 12.45 | 11.40 | 11.13 |
| MnO | 0.21 | 0.23 | 0.21 | 0.14 | 0.19 | 0.22 |
| MgO | 7.64 | 7.47 | 6.90 | 7.07 | 7.22 | 7.05 |
| CaO | 9.51 | 11.47 | 12.08 | 9.71 | 9.16 | 9.33 |
| Na2O | 2.14 | 1.61 | 2.04 | 1.18 | 2.68 | 2.61 |
| K2O | 1.05 | 1.04 | 0.25 | 3.01 | 1.48 | 2.06 |
| P2O5 | 0.45 | 0.45 | 0.20 | 0.47 | 0.41 | 0.34 |
| FeO* | 14.11 | 15.03 | 12.93 | 14.19 | 13.18 | 13.01 |
| Fe2O3/FeO | 0.16 | 0.16 | 0.18 | 0.16 | 0.17 | 0.19 |
| H2O | 2.38 | | 1.76 | 2.45 | 2.15 | 1.54 |
| Rb | 43 | 31 | 80 | 172 | 69 | 119 |
| Ba | 213 | 359 | 363 | 126 | 365 | 152 |
| Sr | 194 | 106 | 162 | 139 | 163 | 100 |
| La | 12 | 13 | 19 | 12 | 9 | 9 |
| Y | 45 | 53 | 44 | 46 | 42 | 46 |
| Th | <2 | 2 | <2 | <2 | <2 | <2 |
| Zr | 206 | 236 | 198 | 213 | 178 | 171 |
| Nb | 11 | 21 | 12 | 11 | 11 | 9.6 |
| Ni | 134 | 107 | 68 | 70 | 90 | 92 |
| V | 308 | 390 | 325 | 346 | 291 | 312 |
| Cr | 281 | 258 | 232 | 202 | 273 | 177 |

| | $G_1$ | | $G_2$ | | $G_3$ | | $G_4$ | | $G_5$ | |
|---|---|---|---|---|---|---|---|---|---|---|
| | C | M | C | M | C | M | C | M | C | M |
| SiO2 | 76.14 | 77.97 | 76.58 | 77.78 | 76.02 | 78.02 | 76.51 | 77.28 | 75.53 | 77.48 |
| TiO2 | 0.14 | 0.13 | 0.14 | 0.14 | 0.15 | 0.14 | 0.13 | 0.13 | 0.14 | 0.16 |
| Al2O3 | 11.52 | 11.61 | 11.55 | 11.77 | 11.51 | 11.49 | 11.48 | 11.23 | 11.74 | 11.59 |
| Fe2O3 | 0.74 | 0.68 | 0.48 | 0.69 | 0.68 | 0.74 | 0.26 | 0.63 | 0.29 | 0.20 |
| FeO | 1.08 | 0.89 | 1.12 | 1.00 | 1.12 | 1.01 | 1.37 | 1.07 | 1.46 | 1.46 |
| MnO | 0.03 | 0.02 | 0.03 | 0.02 | 0.03 | 0.02 | 0.03 | 0.02 | 0.04 | 0.02 |
| MgO | 0.10 | 0.13 | 0.10 | 0.12 | 0.17 | 0.09 | 0.06 | 0.09 | 0.10 | 0.10 |
| CaO | 0.71 | 0.70 | 0.66 | 0.71 | 0.84 | 0.56 | 0.50 | 0.57 | 0.47 | 1.33 |
| Na2O | 3.37 | 6.14 | 2.66 | 5.95 | 3.31 | 5.93 | 2.59 | 3.52 | 2.81 | 5.32 |
| K2O | 4.73 | 0.35 | 4.82 | 0.74 | 4.64 | 0.96 | 5.30 | 4.02 | 5.54 | 0.56 |
| P2O5 | 0.01 | 0.01 | 0.01 | 0.01 | 0.01 | 0.01 | 0.01 | 0.01 | 0.01 | 0.01 |
| FeO* | 1.75 | 1.50 | 1.55 | 1.62 | 1.73 | 1.68 | 1.60 | 1.64 | 1.72 | 1.64 |
| Fe2O3/FeO | 0.69 | 0.76 | 0.43 | 0.69 | 0.61 | 0.73 | 0.19 | 0.59 | 0.20 | 0.14 |
| H2O | 0.33 | 0.16 | 0.39 | 0.30 | 0.28 | 0.12 | 0.35 | 0.19 | 0.40 | 0.36 |
| Rb | 189 | 14 | 190 | 32 | 187 | 31 | 204 | 127 | 223 | 20 |
| Ba | 807 | 177 | 873 | 476 | 867 | 756 | 880 | 1080 | 932 | 344 |
| Sr | 39 | 85 | 49 | 107 | 50 | 62 | 43 | 55 | 43 | 157 |
| La | 63 | 62 | 72 | 68 | 65 | 57 | 58 | 60 | 65 | 63 |
| Y | 72 | 69 | 76 | 77 | 73 | 72 | 69 | 79 | 74 | 64 |
| U | 5 | 5 | 5 | 6 | 5 | 4 | 3 | 7 | 5 | 4 |
| Th | 17 | 15 | 16 | 16 | 17 | 16 | 15 | 13 | 14 | 15 |
| Zr | 232 | 230 | 232 | 230 | 224 | 235 | 217 | 229 | 248 | 238 |
| Nb | 21 | 21 | 20 | 22 | 21 | 20 | 21 | 22 | 22 | 20 |
| Ni | 3 | 2 | 5 | 4 | 4 | <2 | 3 | 3 | <2 | 3 |
| V | <3 | <3 | <3 | <3 | <3 | <3 | <3 | <3 | 3 | 8 |
| Cr | <3 | <3 | <3 | <3 | <3 | <3 | <3 | <3 | <3 | <3 |

Continued table XII.

| | $G_6$ | | $G_7$ | | $G_8$ | |
|---|---|---|---|---|---|---|
| | C | M | C | M | C | M |
| SiO2 | 76.85 | 76.77 | 77.97 | 79.59 | 78.01 | 79.05 |
| TiO2 | 0.14 | 0.15 | 0.13 | 0.13 | 0.12 | 0.13 |
| Al2O3 | 11.71 | 11.78 | 11.66 | 11.44 | 11.73 | 11.74 |
| Fe2O3 | 0.17 | 0.42 | 0.46 | 0.54 | 0.60 | 0.72 |
| FeO | 1.48 | 1.39 | 1.23 | 1.10 | 0.96 | 1.00 |
| MnO | 0.02 | 0.02 | 0.03 | 0.02 | 0.03 | 0.03 |
| MgO | 0.18 | 0.18 | 0.49 | 0.56 | 0.07 | 0.11 |
| CaO | 0.38 | 0.93 | 0.27 | 0.82 | 0.55 | 0.75 |
| Na2O | 2.28 | 5.02 | 2.49 | 4.80 | 2.92 | 5.78 |
| K2O | 5.36 | 1.72 | 5.26 | 0.99 | 4.99 | 0.67 |
| P2O5 | 0.01 | 0.01 | 0.02 | 0.01 | 0.02 | 0.02 |
| FeO* | 1.63 | 1.77 | 1.64 | 1.59 | 1.50 | 1.65 |
| Fe2O3/FeO | 0.11 | 0.30 | 0.37 | 0.49 | 0.63 | 0.72 |
| H2O | 0.70 | 0.32 | 0.64 | 0.35 | 0.14 | 0.23 |
| Rb | 223 | 60 | 149 | 41 | 187 | 25 |
| Ba | 760 | 509 | 759 | 397 | 774 | 573 |
| Sr | 28 | 95 | 37 | 84 | 36 | 83 |
| La | 57 | 56 | 42 | 39 | 54 | 63 |
| Y | 63 | 64 | 62 | 56 | 70 | 68 |
| U | 2 | 4 | 3.13 | 3.74 | 2.63 | 3.70 |
| Th | 13 | 16 | | | | |
| Zr | 235 | 253 | 244 | 251 | 228 | 231 |
| Nb | 21 | 22 | | | | |
| Ni | 5 | 2 | | | | |
| V | <3 | <3 | 23 | 22 | 11 | ≤1 |
| Cr | <3 | <3 | ≤1 | ≤1 | ≤1 | ≤1 |

| | $I_1$ | | $I_2$ | | $I_3$ | |
|---|---|---|---|---|---|---|
| | C | M | C | M | C | M |
| SiO2 | 49.22 | 49.29 | 49.03 | 49.70 | 50.98 | 50.99 |
| TiO2 | 2.77 | 2.80 | 2.58 | 2.86 | 1.90 | 1.98 |
| Al2O3 | 12.55 | 12.62 | 12.72 | 12.48 | 13.31 | 13.61 |
| MnO | 0.31 | 0.31 | 0.20 | 0.20 | 0.24 | 0.23 |
| MgO | 5.28 | 5.24 | 6.11 | 5.33 | 6.70 | 6.70 |
| CAO | 8.92 | 9.00 | 9.40 | 9.10 | 9.16 | 8.80 |
| Na2O | 2.43 | 2.44 | 2.29 | 2.35 | 2.47 | 2.75 |
| K2O | 0.96 | 0.78 | 0.98 | 0.75 | 1.13 | 0.92 |
| P2O5 | 0.45 | 0.49 | 0.29 | 0.34 | 0.16 | 0.21 |
| FeO* | 16.64 | 16.65 | 15.98 | 16.23 | 13.57 | 13.45 |
| Fe2O3/FeO | 0.37 | 0.30 | 0.38 | 0.42 | 0.39 | 0.42 |
| H2O | 0.58 | 1.35 | 1.40 | 1.30 | 1.73 | 1.82 |
| Rb | 33 | 22 | 45 | 25 | 60 | 43 |
| Ba | 196 | 265 | 515 | 372 | 372 | 281 |
| Sr | 112 | 149 | 137 | 141 | 246 | 224 |
| La | 11 | 6 | 9 | 3 | 4 | 4 |
| Y | 42 | 53 | 48 | 50 | 34 | 40 |
| U | 0.674 | 0.741 | 0.474 | 0.309 | 0.240 | 0.163 |
| Zr | 115 | 117 | 130 | 148 | 61 | 86 |
| Nb | 5.3 | 5.3 | 3.7 | 3.9 | 1.4 | 2.1 |
| Ni | 40 | 32 | 59 | 30 | 71 | 68 |
| V | 578 | 589 | 590 | 617 | 470 | 462 |
| Cr | 87 | 56 | 127 | 73 | 139 | 118 |

## REFERENCES


ASKLUND, B., 1950: Kosteröarna, ett nyckelområde för Västra Sveriges Precambriska Geologi. — Sver. geol. unders., C 517, 56 pp.

BEACH, A., 1973: The mineralogy of high-temperature shear zones at Scourie, NW Scotland. — Petrol. 14, 2, 231—248.

— 1976: The interrelations of fluid transport, deformation, geochemistry and heat flow in early Proterozoic shear zones in the Lewisian complex. — Phil. Trans. R. Soc., A 280, 1298, 569—604.

BROOKS, C.K., 1976: The $Fe_2O_3O$/FeO ratio of basalt analysis: an appeal for a standardized procedure. — Bull. geol. Soc. Denmark, 25, 117—120.

BROOKS, C.K. & NIELSEN, T.F.D., 1978: Early stages in the differentiation of the Skaergaard magma as revealed by a closely related suite of dyke rocks. — Lithos, 11, 1—4.

BRYAN, W.B., THOMSON, G., FREY, F.A. & DICKEY, J.S., 1976: Inferred geologic settings and differentiation in basalts from Deep-Sea Drilling Project. — J. Geophys. Res. 81, 4285—4304.

BYERLY, G.R., MELSON, W.G. & VOGT, P.R., 1976: Rhyodacites, andesites, ferro-basalts and ocean tholeiites from the Galapagos spreading centre. — Earth Planet. Sci. Letters, 30, 215—221.

CLARQUE, D.A. & BUNCH, T.E., 1976: Formation of ferrobasalt at East Pacific midocean spreading centres. — J. Geophys. Res. 81, 4247—4256.

COLEMAN, R.G., 1977: Ophiolites. — Springer-Verlag, Berlin.

DALY, J.S., PARK, R.G. & CLIFF, R.A., 1983: Rb-Sr isotopic equilibrium during Sveconorwegian (= Grenville) deformation and metamorphism of the Orust dykes, S.W. Sweden. — Lithos, 16, 307—318.

DE GEER, G., 1899: Om Algonkisk veckning i Fennoskandias gränsområde. — Geol. Fören. Stockh. Förh., 21, 675—693.

— 1902: Beskriftning till kartbladet Strömstad med Koster. — Sver. geol. unders. AC 1.

ELLIOTT, R.B., 1973: The chemistry of gabbro/amphibolite transitions in South Norway. — Contrib. Mineral. Petrol., 38, 71—79.

FIELD, D. & ELLIOTT, R.B., 1974: The chemistry of gabbro/amphibolite transitions in South Norway. — Contrib. Mineral. Petrol., 47, 63—76.

FRATTA, M. & SHAW, D.M., 1974: 'Residence' contamination of K, Rb, Li and Ti in diabase dykes. — Can. J. Earth Sci. 11, 422—429.

GREEN, D.H. & RINGWOOD, A.E., 1967: The genesis of basaltic magmas. — Contrib. Mineral. Petrol. 15, 103—190.

HAGESKOV, B., 1978: On the Precambrian structures of the Sandbukta-Mølen inlier in the Oslo graben, SE Norway. — Norsk Geol. Tidsskr. vol. 58, 69—80.

— 1984: Magnetic susceptibility used in mapping of amphibolite facies recrystallisation in basic dykes. — Tectonophysics 108, 339—351.

— 1985: Constrictional deformation of the Koster dyke swarm in a ductile sinistral shear zone, Koster islands SW Sweden. — Bull. Geol. Soc. Denmark 34, 3—4, 151—196.

HAGESKOV, B. & PEDERSEN, S., 1981: Rb/Sr whole rock age determinations from the western part of the Østfold basement complex, SE Norway. — Bull. Geol. Soc. Denmark 29, 119—128.

HOLM, P.E., 1982: Non-Recognition of Continental Tholeiites using the Ti-Y-Zr Diagram. — Contrib. Mineral. Petrol. 79, 308—310.

JAKES, P. & WHITE, A.J.R., 1972: Major and trace element aboundances in volcanic rocks of orogenic areas. — Bull. Geol. Soc. Am. 83, 29—40.

JAMISON, R.A. & STRONG, D.F., 1981: A metasomatic mylonite zone within the ophiolite aureole, St. Anthony Complex, New Foundland. — Am. J. Sci. 281, 264—281.

KALSBEEK, F., BRIDGWATER, D. & ZECK, H.P., 1978: A 1950±60 Ma Rb-Sr whole-rock isochron age from two Kangamiut dykes and the timing of the Nagssugtoquidian (Hudsonian) orogeny in West Greenland. — Can. J. Earth. Sci. 5, 1122—1128.

KERRICH, R., FYFE, W.S., GORMAN, B.E. & ALLISON, I., 1977: Local modification of rock chemistry by deformation. — Contrib. Mineral. Petrol. 65, 183—190.

LE ROEX, A.P., DICK, H.J.B., REID, A.M., FREY, F.A. & ERLANK, A.J., 1985: Petrology and geochemistry of basalts from the American-Antarctic Ridge, Southern Ocean: implications for westwards influence of the Bovuet mantle plume. — Contrib. Mineral. Petrol. 90, 367—380.

MacDonald, G.A. & Katsura, T., 1964: Chemical composition of Hawaiian lavas. — J. Petrol., 5, 82—133.

Miyashiro, A., 1973: The Trodos ophiolitic complex was probably formed in an Island Arc. — Earth Planet. Sci. Lett. 19, 218—224.

Morthorst, J.R., Zeck, H.P. & Lundegårdh, P.H., 1983: The Proterozoic hyperites in southern Värmland, western Sweden. — Sver. geol. unders. — Ba 30, 1—104.

Norrish, K. & Chappel, B., 1967: X-ray fluorescence spectrography. In Physical methods in determinative mineralogy, 161—214. — Academic Press, London, New York.

Pearce, T.H., 1968: A contribution to the theory of variation diagrams. — Contrib. Mineral. Petrol. 19, 142—157.

Pearce, J.A. & Cann, J.R., 1973: Tectonic setting of basic volcanic rocks determined using trace element analyses. — Earth Planet. Sci. Lett. 9, 290—300.

Rock, N.M.S., McDonald R., Walker, B.H., May, F., Peacock, J.D. & Scott, P., 1985: Intrusive metabasite belts within Moine assemblage, west of Loch Ness, Scotland: Evidence for metabasite modification by country rock infraction. — J. Geol. Soc. London, 142, 643—661.

Shaw, D.M., 1964: A review of K-Rb fractionation trends by covariance analysis. — Geochim. Cosmochim. Acta 33, 573—601.

Starmer, I.C., 1972: The Sveconorwegian regeneration and earlier orogenic events in the Bamble series. — Norges geol. unders. 277, 37—52.

Stout, M.Z. & Nicholls, J., 1977: Mineralogy and petrology of Quarternary lavas from the Snake River Plain, Idaho. — Can. J. Earth Sci. 14, 2140—2156.

Sun, S.S. & Nesbitt, R.W., 1977: Chemical heterogeneity of the Precambrian mantle, composition of the Earth and mantle evolution. — Earth Planet. Sci. Lett. 35, 429—448.

— 1978: Geochemical regularities and genetic significance of ophiolites basalts.- Geology 6, 689–693.

Sørensen, I., 1975: X-ray fluorescence spectrometry at GGU. — Grønlands Geol. Unders. Rapp. 75, 16—18.

— 1976: Progress in calibrating an X-ray spectrometer. — Grønlands Geol. Unders. Rapp. 80, 149—159.

Wager, L.R., 1960: The major element variation of the layered series of the Skaergaard intrusion and a re-estimation of the average composition of the hidden layered series and of successive residual magmas. — J. Petrol. 1, 364—398.

Wooden, L.J., Vitaliano, C.J., Koehler, S.W. & Ragland, P.C., 1978: The late Precambrian mafic dikes of the southern Tobacco Root Mountains, Montana: geochemistry, Rb-Sr geochronology and relationship to belt tectonics. — Can. J. Earth Sci. 15, 467—479.

Yoder, H.S. & Tilley, C.E., 1962: Origin of basaltic magmas; an experimental study of natural and synthetic rock systems. — J. Petrol. 3, 342—532.

Zeck, H.P. & Kalsbeek, F., 1981: Geochemistry of amphibolite facies metamorphism of a suite of basic dykes, Precambrian basement, Greenland. — Chem. Erde. 40, 1—22.

Zeck, H.P. & Morthorst, J.R., 1982: Continental tholeiites in the Ti-Zr-Y discrimination diagram. — N.Jb. Miner. Mh. 5, 193—200.

Zeck, H.P., Shenouda, H.H., Rønsbo, J.G. & Poorter, R.P.E., 1982: Hypersthene-ilmenite(/magnetite) symplectites in coronitic olivine-gabbronorites. — Lithos 15, 173—182.

SGU C 817

# THE KOSTER DYKES

Skarvesätet
Rönningarna
SALTHOLMEN
Valnäsbukten
Hassle-vikarna
NORD-KOSTER
Basteviken
Kostersundet
Huseviksholmen
Hamneholmen
S. Sneholmen
L. Sneholmen
MÖRHOLMEN
Kostersundet
St. Tenholmen
Brand
Kosterhamnen
Hällsholmen
Nypholmen
Eleven
Filjholmen
Jutholmen
Arholmen
SYD-KOSTER
Rundholmen
Måskär
Bockholmen
Tegelholmen
Lådderskären
L. Brattskär
St. Brattskär
Dammstånggrån
Vedskär
BURHOLMEN
St. Korrholmen
Våskär
St. Tjalleskär
RAMSHOLMEN
Sokna
Skåreskär
Inn. Ursholmen
Ytt. Ursholmen
RAMSÖKALVEN
RAMSÖ
Badstugan

0 1 2 KM

SKALA 1:20.000

Godkänd från sekretetssynpunkt för spridning. Lantmäteriverket 1987-06-18

Printed in Sweden by OffsetCenter AB, Uppsala 1987

B Hageskov 1983

PRISKLASS C

Distribution
Liber Distribution
162 89 STOCKHOLM
Tel 08-739 91 30

Fotosats: ORD & FORM AB
Tryck: Offsetcenter ab, Uppsala 1987

ISBN 91-7158-413-7
ISSN 0082-0024